Atmos. Chem. Phys. Discuss., 15, 9445–9505, 2015
www.atmos-chem-phys-discuss.net/15/9445/2015/
doi:10.5194/acpd-15-9445-2015

Atmospheric Chemistry and Physics Discussions

Vertical profiling of aerosol hygroscopic properties in the planetary boundary layer during the PEGASOS campaigns

B. Rosati[1], M. Gysel[1], F. Rubach[2,3,*], T. F. Mentel[2], B. Goger[1,], L. Poulain[3], P. Schlag[2], P. Miettinen[4], A. Pajunoja[4], A. Virtanen[4], J. Bialek[5], H. Klein Baltink[6], J. S. Henzing[7], J. Größ[3], G. P. Gobbi[8], A. Wiedensohler[3], A. Kiendler-Scharr[2], C. O'Dowd[5], S. Decesari[9], M. C. Facchini[9], E. Weingartner[1,***], and U. Baltensperger[1]**

[1]Laboratory of Atmospheric Chemistry, Paul Scherrer Institute (PSI), 5232 Villigen, Switzerland
[2]Institute for Energy and Climate Research (IEK-8), Forschungszentrum Jülich, 52428 Jülich, Germany
[3]Leibniz Institute for Tropospheric Research, 04318 Leipzig, Germany
[4]Department of Applied Physics, University of Eastern Finland, 1627 Kuopio, Finland
[5]School of Physics and Centre for Climate and Air Pollution Studies, National University of Ireland Galway, Galway, Ireland
[6]Royal Netherlands Meteorological Institute (KNMI), 3730 De Bilt, the Netherlands

[7]Netherlands Organization for Applied Scientific Research (TNO), 80015 Utrecht, the Netherlands
[8]Institute of Atmospheric Sciences and Climate (ISAC-CNR), National Research Council, 00133 Rome, Italy
[9]Institute of Atmospheric Sciences and Climate (ISAC-CNR), National Research Council, 40129 Bologna, Italy
[*]now at: Max Planck Institute for Chemistry, 55128 Mainz, Germany
[**]now at: Institute of Meteorology and Geophysics, University of Innsbruck, 6020 Innsbruck, Austria
[***]now at: Institute for Aerosol and Sensor Technology, University of Applied Science Northwestern Switzerland, 5210 Windisch, Switzerland

Received: 26 January 2015 – Accepted: 14 March 2015 – Published: 31 March 2015

Correspondence to: M. Gysel (martin.gysel@psi.ch)

Published by Copernicus Publications on behalf of the European Geosciences Union.

ACPD
15, 9445–9505, 2015

Abstract

Airborne measurements of the aerosol hygroscopic and optical properties as well as chemical composition were performed in the Netherlands and northern Italy on board of a Zeppelin NT airship during the PEGASOS field campaigns in 2012. The vertical changes in aerosol properties during the development of the mixing layer were studied. Hygroscopic growth factors (GF) at 95 % relative humidity were determined using the white-light humidified optical particles spectrometer (WHOPS) for dry diameters of 300 and 500 nm particles. These measurements were supplemented by an aerosol mass spectrometer (AMS) and an aethalometer providing information on the aerosol chemical composition.

Several vertical profiles between 100 and 700 m a.g. were flown just after sunrise close to the San Pietro Capofiume ground station in the Po Valley, Italy. During the early morning hours the lowest layer (newly developing mixing layer) contained a high nitrate fraction (20 %) which was coupled with enhanced hygroscopic growth. In the layer above (residual layer) small nitrate fractions of ~ 2 % were measured as well as low GFs. After full mixing of the layers, typically around noon and with increased temperature, the nitrate fraction decreased to 2 % at all altitudes and led to similar hygroscopicity values as found in the residual layer. These distinct vertical and temporal changes underline the importance of airborne campaigns to study aerosol properties during the development of the mixed layer. The aerosol was externally mixed with 22 and 67 % of the 500 nm particles in the range $GF < 1.1$ and $GF > 1.5$, respectively. Contributors to the non-hygroscopic mode in the observed size range are most likely mineral dust and biological material. Mean hygroscopicity parameters (κ) were 0.34, 0.19 and 0.18 for particles in the newly forming mixing layer, residual layer and fully mixed layer, respectively. These results agree well with those from chemical analysis which found values of $\kappa = 0.27$, 0.21 and 0.19 for the three layers. The highest κ values in the new mixed layer and lower values in the fully developed mixed layer were additionally confirmed by ground measurements.

ACPD
15, 9445–9505, 2015

The aerosol sampled in the Netherlands did not show any altitude dependent characteristics because only the fully mixed layer or the entrainment zone between mixed and the residual layer were probed. The airborne hygroscopicity measurements agreed well with ground based composition measurements. However, the fraction of the hygroscopic particles (GF > 1.5) was enhanced compared to the results from Italy amounting to 82 %, while 12 % showed low hygroscopicity (GF < 1.1). The mean κ value measured by the WHOPS was 0.28 and therefore considerably higher than the value measured in the fully mixed layer in Italy.

The effective index of refraction reached values of 1.43 and 1.42 for the 500 nm particles in Italy and the Netherlands, respectively. This coincides well with literature data for airmasses with predominant organic contribution as was the case during our flights.

1 Introduction

Aerosol particles can directly have an impact on climate by absorbing or scattering the solar radiation. The optical properties depend on the particles' size as well as their chemical composition and can be altered at elevated relative humidities (RH) if the particles are hygroscopic (IPCC, 2013).

Most particles are emitted or formed in the planetary boundary layer (PBL), which describes the lowermost layer of the troposphere. The PBL is subject to many changes depending on the strength of the incident solar radiation (see Stull, 1988 for more information on the PBL): Under clear conditions heating of the Earth's surface by solar radiation induces convective turbulence and therefore a well-mixed PBL builds up after midday ranging up to an altitude of approximately 2 km. During night when the surface cools down, several sub-layers are present in the PBL where the upper most part is defined as the residual layer (RL). The RL contains a mixture of emissions and background aerosol from the day before and is decoupled from the surface. Close to the ground a stable nocturnal layer (NL) develops where local and/or regional emissions

ACPD
15, 9445–9505, 2015

can accumulate. Once the sun rises a new mixing layer (ML) is formed which is separated from the other layers through a temperature inversion. Throughout the day this ML evolves until it reaches up to the free troposphere. The dynamics of the sub-layers in the PBL and the properties of the aerosol particles in these layers are still poorly understood.

Airborne studies were previously performed to investigate the aerosol chemical composition as a function of altitude utilizing an aerosol mass spectrometer (AMS), showing that chemical composition varies with height (Morgan et al., 2009, 2010a, b; Pratt and Prather, 2010). This variation should influence the particles' hygroscopic growth. Morgan et al. (2010a) conducted flights over north-western Europe, concentrating however on changes between 0 and 10 km a.g. In general aircraft campaigns commonly stretch over large horizontal and vertical ranges, therefore providing only limited information on the PBL. On the other hand, ground based studies have directly investigated the hygroscopic properties of particles. However, surface measurements are not always representative for aerosol properties at elevated altitudes. In addition, hygroscopic properties of particles are studied in reaction chambers under controlled conditions (e.g. Duplissy et al., 2011, or Tritscher et al., 2011).

One way to explore the hygroscopic properties of aerosols is to measure the so called hygroscopic growth factor (GF) defined as the ratio of the particle diameter D_{wet} at a certain relative humidity (RH) divided by its dry diameter D_{dry}:

$$\mathrm{GF(RH)} = \frac{D_{\mathrm{wet}}(\mathrm{RH})}{D_{\mathrm{dry}}} \quad (1)$$

The most common instrument for ground-based hygroscopicity measurements of atmospheric aerosol particles is the hygroscopicity tandem differential mobility analyzer (HTDMA; see e.g. Liu et al., 1978, or McMurry and Stolzenburg, 1989, for details). It explores particles in the sub-saturated RH range and was employed successfully in several ground based campaigns (a review is presented in Swietlicki et al., 2008). This method investigates GFs at high precision but needs several minutes for a full

ACPD
15, 9445–9505, 2015

measurement cycle which makes it rather unsuited for airborne measurements. Besides, its detection range is limited to a maximal dry mobility diameter of approximately 250 nm.

HTDMA and chemical composition hygroscopicity closures were performed at various sites including urban (see e.g. Kamilli et al., 2014) but also rural regions (see e.g. Wu et al., 2013). Altitude dependent hygroscopic properties were investigated by employing HTDMAs at elevated mountain sites, like the Jungfraujoch (e.g. Kammermann et al., 2010) or Puy de Dôme (e.g. Holmgren et al., 2014), however these measurements may be influenced by surface emissions and cannot provide a detailed analysis of particles at different elevations.

To our knowledge, only few campaigns report airborne hygroscopicity results due to the lack of available instruments suited for this kind of measurements. The first instrument built for this special task is the differential aerosol sizing and hygroscopicity spectrometer probe (DASH-SP; Sorooshian et al., 2008). It is constructed using a combination of differential mobility analysis (DMA) and optical particle spectrometry (OPS) and has successfully been applied for airborne GF measurements at sub-saturated RH. This instrument focuses on small sizes in the range of 150–225 nm dry diameters. Results are reported for aircraft campaigns in Hersey et al. (2009) and Hersey et al. (2013). In these studies an attempt was made to reconcile simultaneously measured chemical composition using an AMS and GF results. Hersey et al. (2009, 2013) focused their studies on the free troposphere in the marine atmosphere off the coast of California.

All measurement techniques mentioned so far to study hygroscopicity focus on particles smaller than ∼ 300 nm which implies that species that are more abundant at larger sizes (e.g. sea salt, mineral dust) cannot be fully investigated. This may induce an underestimation of the scattering potential of the overall aerosol particles but also an underestimation of the overall hygroscopic properties of atmospheric aerosol particles. Zieger et al. (2011) presented a comparison between HTDMA measurements for dry diameters of 165 nm and calculated GFs using size distributions, scattering

ACPD
15, 9445–9505, 2015

enhancement factors (based on polydisperse aerosol particles) and Mie theory. The comparison revealed that indeed in the presence of sea salt the HTDMA results were not representative for the atmospheric particles, finding too small GF values. Based on these findings we concluded that studies of hygroscopic properties of larger sizes are needed in order to get a more complete picture of the ambient aerosol particles. Hence, we developed the white-light humidified optical particle spectrometer (WHOPS; Rosati et al., 2015) to perform vertical profiles of the particles' hygroscopic properties of optically more relevant sizes (D_{dry} = 300, 500 nm).

Within the Pan-European Gas–AeroSOl-climate interaction Study (PEGASOS) air-masses over Europe were explored in order to understand feedbacks between atmospheric chemistry and a changing climate. A Zeppelin NT ("New Technology") was chosen as measurement platform to specifically probe changes in different layers present in the evolving convective PBL. The WHOPS, together with an aethalometer and an AMS were mounted in the Zeppelin NT airship to investigate GFs and chemical composition. In the current study, data from vertical profiles measured above central (Cabauw, Netherlands) and southern Europe (Po Valley, Italy) are presented (Fig. 1 shows the campaign locations). Flight data is further compared to results from ground measurements to get a complete picture of the dynamics and altitude dependent aerosol properties. Additionally, the hygroscopic mixing state and the effective index of refraction of the particles are explored.

2 Experimental

2.1 The Zeppelin NT airship

The Zeppelin NT airship, which served as a platform for the airborne measurements, flew with an average speed of 50 km h^{-1} a.g. and reached altitudes between 80 and approximately 1000 m a.g., depending on the pay load and ambient temperature. Therefore a good spatial and temporal resolution of the gas-phase and aerosol properties

ACPD
15, 9445–9505, 2015

could be obtained. Additionally, the Zeppelin characteristics allowed for a distinct focus on the evolution of the mixed layer forming at low altitudes in the first hours of sunlight. For flight safety reasons, the Zeppelin could only be deployed on days with low wind speeds, low cloud coverage or clear sky.

The Zeppelin NT airship could be equipped with different instrumental layouts for focusing on certain research questions. For this study the so called secondary organic aerosol (SOA) layout was utilized. This layout focuses on the measurement of aerosol properties like aerosol hygroscopicity, size distribution, particle number concentration, chemical composition and volatile organic compounds (VOC). The specific instruments used to measure these properties are described in the following subsections. In addition, nitrogen oxides (NO_x), ozone (O_3), carbon monoxide (CO), radiative flux, hydroxy as well as peroxy radicals (OH, HO_2) were monitored continuously on board of the airship. Each instrument had a separate inlet system and a separate sampling position.

2.2 Flight and ground based measurement locations

2.2.1 Po Valley site

The Italy campaign, within the PEGASOS project, was located in the Po Valley, a region known for its remarkably high air pollution levels, compared to other places in Europe (see e.g. Putaud et al., 2010). The Po Valley hosts several industrial, urban and agricultural areas allowing for detailed anthropogenic pollution studies, however also long-range transport and aged aerosol from other sites can be investigated. The Zeppelin NT airship was stationed at Ozzano Airport (located at 44°28′ N, 11°32′ E, ∼ 30 km southeast of Bologna) and performed flights during June and July 2012 in the greater Po Valley region. The vertical profiles were focused above the San Pietro Capofiume (SPC) ground station (located at 44°39′ N, 11°38′ E), a rural background site which lies approximately 40 km north-east of Bologna. Additionally, data from Monte Cimone (MTC), a mountain site located at 2165 m a.s.l. approximately 100 km south-west of SPC is included in the analysis presented here to complement the airborne data with

ACPD
15, 9445–9505, 2015

results measured at an elevated site. Throughout the PEGASOS campaign the SPC and MTC station were equipped with a set of instruments equivalent to those on the Zeppelin NT airship in order to compare flight and ground level data. In order to get estimates of the mixing layer height a Jenoptik CHM15K "Nimbus" automated Lidar-ceilometer was employed at SPC (e.g., Angelini et al., 2009, Haeffelin et al., 2012 and Di Giuseppe et al., 2012).

2.2.2 Netherlands site

The campaign in the Netherlands was located in the South Holland and Utrecht region. This region is representative for north-west Europe and is influenced by continental and maritime airmasses, depending on the wind direction. The Zeppelin NT airship was stationed at Rotterdam – the Hague Airport and conducted several flights in May 2012. The vertical profiles were performed near the Cabauw Experimental Site for Atmospheric Research (CESAR, located at 51°97′ N, 4°93′ E). The CESAR station hosts a number of instruments to characterize radiative properties, climate monitoring and atmospheric processes (www.cesar-observatory.nl). During the PEGASOS campaign an aerosol mass spectrometer was added to the permanently installed aerosol measurements. Also at this station a ceilometer system (Vaisala LD40) was utilized to get an estimated mixing layer height (Haij et al., 2007).

2.3 Instrumentation for aerosol measurements

2.3.1 Hygroscopic and optical aerosol properties

On the Zeppelin the hygroscopic and optical properties were measured using the white-light humidified optical particle spectrometer (WHOPS). The WHOPS and associated calibration and data analysis procedures are described in detail in Rosati et al. (2015). Briefly, particles reach the WHOPS and are dried in a diffusion drier and then size selected in a differential mobility analyzer (DMA). In the next step these particles are

ACPD
15, 9445–9505, 2015

either guided directly to a WELAS 2300 optical particle spectrometer (WELAS; Palas GmbH, Karlsruhe, Germany) for a measurement of the particle size distribution (~ 300–10 000 nm) or humidified in-between. Hygroscopicity measurements are typically performed at RH = 95 %, where the uncertainty in the humidity measurement is assumed to be ±2 %. Since the RH to which particles were exposed to varied only between ~ 94–96 % during both flight days, no further RH corrections were applied to the results. By measuring at both conditions an optically measured size distribution for the size-selected particles can be recorded in their dry and humidified state.

To be able to link the measured partial scattering cross sections (σ; from now on referred to as simply scattering cross section) of the WELAS to specific geometric diameters several factors have to be known: the index of refraction (m) as well as the optical setup of the instrument, the spectrum of the light source and sensitivity of the detector. This specific optical instrument was chosen because it uses a white-light source (OSRAM XBO-75 Xenon short arc lamp) which minimizes Mie oscillations for the light scattering which in turn allows for mostly unambiguous attribution of particle diameter to measured scattering cross section. Once a specific dry mobility diameter is selected, the optically measured σ can be converted to optical diameters (D) using a σ-D-m table for a series of different indices of refraction calculated with the Mie code (Mie, 1908; Bohren and Huffman, 2007). The index of refraction where the optical diameter of the dry particles coincides with the selected mobility diameter is then defined as the effective index of refraction (m) of the dry particles. The term "effective" refers to the fact that only the real part can be derived and that particles are assumed to be spherical for all calculations. During the measurement campaigns the instrument was periodically checked and calibrated with well defined aerosols with known optical properties and hygroscopicity, e.g. ammonium sulfate particles.

Figure 2 illustrates the temporal variability of the observed effective index of refraction m for the described flights on 20 June 2012 in the Po Valley and 24 May 2012 in the Netherlands. It has to be noted that only the results for a dry selected mobility diameter of 500 nm are shown. In Italy a mean m_{dry} of 1.43 ± 0.02 (mean ± SD) and

ACPD
15, 9445–9505, 2015

in the Netherlands $m_{dry} = 1.42 \pm 0.02$ were found. However, an absolute uncertainty of ±0.04 has to be attributed to all index of refraction retrievals (see Rosati et al., 2015). This range compares well to former laboratory studies for SOA from biogenic sources which present values between 1.44–1.45 (Kim and Paulson, 2013; Wex et al., 2009). Guyon et al. (2003) performed ambient aerosol measurements in the Amazon background atmosphere and found also similar values of 1.42 (at $\lambda = 545$ nm) for airmasses dominated by organics. In contrast airmasses with predominant anthropogenic pollution would reach higher indices of refraction of approximately 1.50–1.55 (Ferrero et al., 2014; Yamasoe et al., 1998). The low indices of refraction found in this study from the WHOPS results fit well to the strong contribution of organics to the total aerosol mass concentration measured by the AMS as will be discussed in more detail later.

The SPC and MTC sites were equipped with hygroscopicity tandem differential mobility analyzers (HTDMA; see e.g. Swietlicki et al., 2008) where the hygroscopic properties of particles with dry diameters between 35 and 230 nm were measured. The setup comprises two DMAs connected in series combined with a condensation particle counter (CPC). First a monodisperse aerosol is selected in the first DMA, then exposed to elevated relative humidity (typically 90 %) and the resulting size distribution is then measured using a DMA coupled to a CPC providing a GF distribution. The inversion of the HTDMA results was done with the algorithm proposed by Gysel et al. (2009). For a direct comparison to the WHOPS measurements the HTDMA GF-probability density functions (GF-PDF) were recalculated for RH = 95 % using Eq. (5) in Gysel et al. (2009). Note that the dry sizes selected by the WHOPS are larger compared to those selected by the HTDMAs, which focus on smaller particles.

2.3.2 Aerosol chemical composition

A high resolution time-of-flight aerosol mass spectrometer (HR-ToF-AMS; DeCarlo et al., 2006) was employed to characterize the non-refractory chemical composition of aerosol particles. The term non-refractory refers to all species that flash vaporize at 600 °C and $\sim 10^{-7}$ Torr. Aerosols pass a critical orifice and an aerodynamic lens

ACPD
15, 9445–9505, 2015

which focuses particles of sizes between 100 and 700 nm into a narrow beam. The particle beam is impinging on a hot surface (600 °C), where the non-refractory components flash vaporize. The resulting vapors are ionized by electron impact ionization and measured with a time-of-flight mass spectrometer. The high mass spectral resolution of the employed mass spectrometer allows for identification and quantification of peaks corresponding to classes of chemical species (e.g. nitrates, sulphates, chloride, ammonia and organics). Where mass resolution is not sufficient or more than one chemical species fragments to the same ion in the ionization process, known relationships between peaks at different mass to charge ratios are used to improve quantification (fragmentation table, Allan et al., 2004). Two operational modes of the ToF-MS (V- and W-Mode) were used during the flights. Specifications of the adaptation of the HR-ToF-AMS for the Zeppelin requirements can be found in Rubach (2013). A collection efficiency (CE) of 1 was applied to the AMS measurements, based on a comparison between mass concentrations derived from particle size distributions measured by scanning mobility particle sizers (SMPS; TSI Inc., DMA Model 3081 and water – CPC Model 3786) and WELAS, and the results of AMS and aethalometer measurements on the Zeppelin. Because a CE of 1 is higher than observed in other field studies and we cannot explain the differences, we must attribute an uncertainty of ∼ 50 % for the Zeppelin AMS mass concentrations. The same procedure was applied to the ground measurements at SPC yielding the same conclusion that a CE of 1 has to be used. In Cabauw the CE was corrected using the algorithm proposed by Middlebrook et al. (2012). The mass fractions of the compounds are independent of this uncertainty.

At the ground stations, both in Italy and the Netherlands, equivalent black carbon (eBC) mass concentrations were measured with a multi-angle absorption photometer (MAAP Thermo Scientific Model 5012; Petzold et al., 2005) with a resolution of five minutes and an uncertainty of 12 % (Petzold and Schönlinner, 2004). A mass absorption cross section (MAC) of 6.6 $m^2 g^{-1}$ for a wavelength of 637 nm (Müller et al., 2011) was chosen to convert the signal into eBC mass concentrations. A portable aethalometer (AE42, MAGEE Scientific; Berkeley, USA) was mounted on the Zeppelin NT to monitor

ACPD
15, 9445–9505, 2015

the eBC mass concentrations. Results at a wavelength of 880 nm were used. During the flights a maximal attenuation of 70 % and a 4 L min^{-1} flow were chosen. The data was used as retrieved by the manufacturers' firmware using an apparent MAC of 16.6 m^2 g^{-1} at a wavelength of 880 nm, which, however, contains already a correction for the multiple scattering in the filter matrix. In order to get comparable eBC values from MAAP and aethalometer, both instruments should use the same MAC value. A comparison to the MAAP shows that the aethalometer multiple scattering correction factor C (Weingartner et al., 2003) is 3.48 (assuming to be wavelength independent). This value fits relatively well to previous results found at the rural background site of Cabauw of 4.09 by Collaud Coen et al. (2010). As the AMS roughly measures particles smaller than 1 µm and most of eBC is assumed to be present in the size range below 1 µm we refer to the chemical composition as of PM_1 (particulate mass with an aerodynamic diameter smaller than 1 µm) in the following.

3 κ-Köhler theory

In order to link hygroscopicity measurements made at different RH using different instruments, it is common to use the semi-empirical κ-Köhler theory introduced by Petters and Kreidenweis (2007):

$$\mathrm{RH_{eq}}(D_{\mathrm{dry}}, \mathrm{GF}, \kappa) = a_{\mathrm{w}}(\mathrm{GF}, \kappa) \cdot S_{\mathrm{k}}(\mathrm{GF}, D_{\mathrm{dry}}) = \frac{\mathrm{GF}^3 - 1}{\mathrm{GF}^3 - (1-\kappa)} \cdot \exp\left(\frac{4\sigma_{\mathrm{s/a}} M_{\mathrm{w}}}{RT\rho_{\mathrm{w}} D_{\mathrm{dry}} \mathrm{GF}}\right) \quad (2)$$

Köhler theory relates the equilibrium RH ($\mathrm{RH_{eq}}$) over a solution droplet to the product of the water activity a_{w} representing the Raoult term, and factor S_{k} representing the Kelvin term. D_{dry} describes the dry diameter, GF the growth factor (see Eq. 1), $\sigma_{\mathrm{s/a}}$ is the surface tension of the solution/air interface, M_{w} the molecular mass of water, R the ideal gas constant, T the absolute temperature and ρ_{w} the density of water. κ is the semi-empirical hygroscopicity parameter introduced by Petters and Kreidenweis (2007), which captures the composition dependence of the Raoult term.

ACPD
15, 9445–9505, 2015

To derive κ values from GF measurements at specific RHs, the relation between a_w and GF as described by Petters and Kreidenweis (2007) is used:

$$\kappa_{meas} = \frac{(GF(RH)^3 - 1) \cdot (1 - a_w)}{a_w} \quad (3)$$

The subscript "meas" refers to the fact that this κ value is based on the measured GF. The water activity can be inferred from the RH and equilibrium droplet diameter (D_{wet}):

$$a_w = \frac{RH}{\exp\left(\frac{4\sigma_{s/a} M_w}{RT\rho_w D_{wet}}\right)} \quad (4)$$

In our calculations the surface tension of water is assumed. For a composition-hygroscopicity closure, the κ values derived from the GF measurements (WHOPS) as described above are compared with the κ values derived from the chemical composition measurements (AMS and aethalometer). The κ values of a mixed particle, κ_{mix}, can be estimated from the pure component behavior using the Zdanovskii, Stokes and Robinson (ZSR; Stokes and Robinson, 1966) mixing rule. According to the ZSR mixing rule, κ_{mix} is simply the volume fraction weighted mean of the κ values, κ_i, of all components in pure form (Petters and Kreidenweis, 2007):

$$\kappa_{mix} = \sum_i \epsilon_i \kappa_i \quad (5)$$

Where ϵ_i is the volume fraction of component i in the mixed particle.

The mass concentrations of nitrate, sulfate, ammonia, organics and chloride ions as measured by the AMS were converted to neutral salts in order to apply Eq. (5) to calculate hygroscopic properties of the aerosol particles. To do so the ion paring mechanism described by Gysel et al. (2007) in their Eq. (2) was used. The corresponding

ACPD
15, 9445–9505, 2015

densities as well as κ values for the corresponding pure compounds for the prediction of the hygroscopicity parameter are summarized in Table 1. For the inorganic salts, the bulk densities were taken from literature and the κ values were derived from AD-DEM predictions (Topping et al., 2005) which is a detailed model capable of calculating growth factors of inorganic aerosols with high accuracy. The final κ values were calculated for 95 % RH and a dry diameter of 500 nm. For the organics a κ value of 0.11 was used. This was inferred from the median O : C ratio of 0.5 measured during the flights and Fig. 7 in Duplissy et al. (2011), assuming that the organics measured in our studies behaved like organics in previous measurement campaigns and like secondary organic aerosol derived from the oxidation of α-pinene. To determine the organic's density a parametrization based on O:C and H:C ratios introduced by Kuwata et al. (2012) was used. The mean organics' density and SD was found to be $1233 \pm 35\,\mathrm{kg\,m^{-3}}$. eBC was assumed to have $\kappa = 0$ and a bulk density of $2000\,\mathrm{kg\,m^{-3}}$.

4 Results and discussion

4.1 Po Valley campaign

Here we present hygroscopicity results recorded with the WHOPS aboard the Zeppelin NT airship. The vertical flight pattern performed on the 20 June 2012 is shown in Fig. 3. During this day vertical profiles were measured near the SPC site from ~ 08:30 LT until approximately 14:00 LT with a refuel break in-between (~ 10:00–11:00 LT). Two different height levels were covered at approximately 100 and 700 m a.g. On this day westerly winds and wind speeds around $2–3\,\mathrm{m\,s^{-1}}$ prevailed. Therefore the airmasses originated from the Po Valley plain and due to the low wind speeds the influence of local pollution was highest. Figure 3 depicts the potential temperature (Θ) and RH profiles during the flight together with the estimated mixing layer height provided by Ceilometer-Lidar data. The RH ranges from 30 % to a maximum of 60 % and shows a clear altitude dependence: during the first part of the flight the RH was always higher

ACPD
15, 9445–9505, 2015

near the ground, while later in the day the opposite trend is visible. The evolutions of Θ and RH elucidate a clear layering during the beginning of the flight (seen as abrupt change in Θ between 100 and 700 m a.g.), which slowly disappears towards the last profiles. This development is also consistent with the evolution of the estimated mixing layer height, which indicates that during the morning hours (∼ 08:30–10:00 LT) we were able to ascend into the RL and investigate the new ML at the lower altitudes. During the second half of the flight (∼ 12:00–14:00 LT) the fully developed ML was probed at both altitudes.

4.1.1 Hygroscopic GF measured with the WHOPS

Figure 4 gives an overview of the flight day complemented by the time series of the hygroscopicity parameters deduced from the WHOPS measurements (colored in violet). The shaded area describes the accuracy of the WHOPS of 10 % (see Rosati et al., 2015 for more details). Variations of the particles' hygroscopic properties can be observed as a function of altitude and time: The first two height profiles (∼ 08:30–10:00 LT; from now on referred to as IHP1/2), depict higher hygroscopicity values close to the ground (∼ 100 m a.g.) compared to those at elevated altitudes of ∼ 700 m a.g. This altitude dependence implies different layers with distinct aerosol properties, consistent with the vertical layering of the PBL suggested by Θ and the estimated mixing layer height illustrated in Fig. 3. Table 2 contains the mean GF(95 %) and κ values for both layers, averaged over both profiles. In the new ML the mean GF(95 %) is 1.88 which is equivalent to $\kappa = 0.34$. These values considerably exceed the results in the RL (GF(95 %) = 1.61 and $\kappa = 0.19$). After 11:00 LT a second set of profiles was performed. To study particles in the fully developed ML the results from IHP4/5/6 (∼ 12:00–14:00 LT) are considered, while IHP3 is excluded since the ML was not fully developed before noon (see Fig. 4). In the fully developed ML, hygroscopicity results show less variability with no clear pattern for results at different altitudes. We observed one event at around 12:45 LT and 100 m a.g., when the mean κ was considerably lower. This could be explained by the presence of an aerosol layer which contained particles with

ACPD
15, 9445–9505, 2015

a much lower hygroscopicity compared to particles measured before and after. With exception of this instance, the particle hygroscopic properties were homogeneous across all altitudes in the afternoon. This is in concordance with the findings from Θ and the estimated mixing layer height displayed in Fig. 3 which indicate the presence of only one layer below ∼ 700 m a.g. Once the fully developed ML is present vertical differences in aerosol properties are expected to disappear. Only altitude dependent changes in temperature and RH could potentially lead to alterations of the particles e.g. through phase partitioning effects. Mean GF and κ values at different altitudes in the fully developed ML, presented in Table 2, show less spread with values of 0.14 and 0.21 at 100 and 700 m a.g., respectively. The discrepancy can be attributed to the outlier described above which causes a decreased mean value at an altitude of ∼ 100 m a.g., however the results still agree within the measurement accuracy. In addition, the hygroscopic properties in the fully developed ML appear very similar to those measured in the RL.

4.1.2 Mixing state inferred from WHOPS measurements

The GF-PDFs of the humidified particles can provide information on the mixing state of particles with respect to aerosol components of different hygroscopicity. Commonly the mixing state of aerosol particles is classified as follows: if all particles of a certain size have almost the same chemical composition, they are described as internally mixed, whereas if particles of equal size have different chemical composition, they are referred to as externally mixed. Depending on the mixture the hygroscopic behavior will change: internally mixed aerosols will grow uniformly with increasing RH, while external mixtures of substances with differing hygroscopic properties will result in multimodal and/or broadened GF-PDFs.

In order to further explore differences in hygroscopic properties between the different layers, Fig. 5 illustrates the GF-PDFs averaged for the same layers, i.e. the same times and altitudes, as the mean values shown in Table 2. In general broad GF(95 %) distributions with values between 0.9 and ∼ 2.5 were observed independently of flight altitude or time of day, hence in all four panels of Fig. 5. Vertical differences can be

ACPD
15, 9445–9505, 2015

observed for the PDFs during IHP1/2 (Fig. 5a and c). The fraction of more hygroscopic particles (GF > 1.5) is more pronounced in the new ML, while the fraction of particles with GF < 1.1 is higher in the RL. This explains the higher mean particle hygroscopicity in the new ML compared to the RL.

In the early afternoon, the GF-PDFs measured during IHP4/5/6 do not exhibit any clear vertical differences (Fig. 5b and d), supporting the above finding of being within the fully developed ML at both altitudes. Subtle differences are a slightly higher fraction of particles with GF < 1.1 and a slightly lower fraction of particles with GF > 1.5 at 100 m a.g. compared to 700 m a.g. This difference is for the most part caused by the outlier at ~ 12:45 LT, as will be shown below with Fig. 6. When comparing the results at fixed elevation at different times (Fig. 5a vs. b and c vs. d as well as Fig. 4) distinct changes were only observed at the lower altitude in the transition from the new ML to the fully developed ML, while little changed at the higher altitude in the transition from the RL to the fully developed ML. This indicates that local aerosol sources have a stronger influence in the shallow new ML, while the fully developed ML is dominated by background aerosol.

Figure 5 illustrates qualitative differences for distributions which were averaged over a certain time period. Even though the GF-PDFs imply externally mixed aerosol particles, this is not necessarily the case as the average of an internally mixed aerosol with variable composition could potentially yield the same result. Due to low counting statistics highly time resolved GF-PDFs are not available. For this reason we divide the particles in different hygroscopic fractions in order to further investigate the time dependent mixing state characteristics. Measurements for D_{dry} = 500 nm are classified in three hygroscopicity categories: GF < 1.1 ("non-hygroscopic"), 1.1 < GF < 1.5 ("moderately hygroscopic") and GF > 1.5 ("most hygroscopic") which correspond to ranges of $\kappa < 0.02$, $0.02 < \kappa < 0.13$ and $\kappa > 0.13$, respectively. Figure 6 presents the temporal evolution of the number fractions of particles in these three categories together with the flight altitude. At all times, particles are simultaneously present in at least two, mostly all three hygroscopicity ranges, which indicates an externally mixed aerosol throughout

ACPD
15, 9445–9505, 2015

the flight. The moderately hygroscopic particles are almost always the smallest fraction, constantly accounting for less than 20 % of all particles (light blue dots in Fig. 6).The most hygroscopic particles are almost always the largest fraction, accounting for ~ 45–85 % of all particles, while the non-hygroscopic particles contribute ~ 9–34 %, whereby these values do not include the outlier. It is important to note that part of the temporal variability of the number fractions shown in Fig. 6 is caused by limited counting statistics rather than true variability of aerosol properties. However, the outlier in the fully developed ML at 12:45 with a non-hygroscopic fraction as high as 50 %, reflects truly different aerosol properties rather than just statistical noise.

Previous mixing state studies, based on hygroscopic growth behavior measured with HTDMAs, found similar substantial non-hygroscopic fractions in airmasses influenced by urban areas, where externally mixed black carbon (BC) was revealed as the major contributor (see e.g. Juranyi et al., 2013; Laborde et al., 2013; Lance et al., 2013). The number size distributions of freshly emitted BC particles typically peak in the range around ~ 100 nm (Rose et al., 2006). Therefore, externally mixed BC is less likely to give a significant contribution to the total number of particles with a diameter of 500 nm, which is probed by the WHOPS, while substantial contributions from externally mixed BC can be expected in the lower accumulation mode size range probed by e.g. HTDMAs, when being close to sources. Besides, externally mixed BC particles are known to have a low effective density due to their fractal-like morphology (Weingartner et al., 1997), and the index of refraction of BC differs substantially from that of organic and inorganic aerosol components (Bond and Bergstrom, 2006). These two effects, lead to a systematic bias in the GF inferred from WHOPS measurements of externally mixed BC particles. Sensitivity analysis showed that it is very unlikely that non-hygroscopic externally mixed BC shows up at GF ~ 1.0 in the WHOPS, despite the fact that the two effects counteract each other to some extent. BC-containing particles may potentially grow into the size range probed by the WHOPS through atmospheric aging processes, i.e. the acquisition of condensable vapors forming a shell around the BC core. This can result in large accumulation mode particles enriched in BC as previously found in

ACPD
15, 9445–9505, 2015

the Po Valley by Decesari et al. (2014). The acquisition of coatings also increases the effective density of BC-containing particles and makes their effective index of refraction more similar to that of BC-free particles (Zhang et al., 2008), however, the hygroscopicity increases as well (e.g. Tritscher et al., 2011; Laborde et al., 2013). Thus, internally mixed BC-containing particles may give a significant contribution to particles with diameters of ∼ 500 nm, however, they are expected to be moderately hygroscopic and they should be detected as such by the WHOPS. Based on the above arguments, we consider it unlikely that the non-hygroscopic particles measured by the WHOPS are for the most part BC-containing particles. Besides, non-BC products of biomass burning, like tar balls (Pósfai et al., 2004; Alexander et al., 2008) are also known to exist up to diameters of ∼ 500 nm. Their optical properties differ significantly from those of BC leading to scattering cross sections similar to those for particles with $m = 1.43$ (effective index of refraction measured in this study). Therefore, also these tar balls could describe a fraction of the non-hygroscopic particles.

Mineral dust is another substance known to be non-hygroscopic (e.g. Herich et al., 2008, 2009), though it can potentially become more hygroscopic through atmospheric aging processes such as e.g. heterogeneous chemical reactions at the particle surface (Vlasenko et al., 2006). Fresh Saharan dust sampled at Cape-Verde was related to the non-hygroscopic particle mode (Schladitz et al., 2011). Aged Saharan dust, observed at the high-alpine site Jungfraujoch after long-range transport, was still reported to be non-hygroscopic using HTDMA and humidified nephelometry techniques (Sjogren et al., 2008; Fierz-Schmidhauser et al., 2010). The number size distribution of mineral dust particles is known to extend down to sub-micrometer sizes (e.g. Mahowald et al., 2014) and therefore into the range of the WHOPS measurements. The hygroscopic growth factor of externally mixed dust particles could hypothetically explain our non-hygroscopic fraction. Dust particles have an index of refraction that is approximately $1.53 - 0.08\,i$ (Wagner et al., 2012), thus leading to similar scattering cross sections at $D_{dry} = 500$ nm as for the effective index of refraction determined for the whole aerosol population ($m = 1.43$). Influence of Saharan dust intrusions all the way down

ACPD
15, 9445–9505, 2015

to the lowest atmospheric layers near the SPC site can be expected for the day of the Zeppelin flight reported here according to the HYSPLIT model for Saharan Dust Intrusions (http://www.ciecem.uhu.es/hysplit/; not presented here). Thus, mineral dust is a likely explanation for the non-hygroscopic particles (at D_{dry} = 500 nm) detected by the WHOPS in the Po Valley.

A last potential candidate for non-hygroscopic particles is biological material, which is non-hygroscopic and exists in the sub-micron size range (e.g. Després et al., 2012). Virus particles, bacteria, fungal spores and plant pollen are commonly ranked among these species. The optical properties vary considerably between different types of bio-aerosol. Values between 1.397–1.53 for the real part of the index of refraction are reported in the literature (Balaev et al., 2003; Charrière et al., 2006; Limsui et al., 2008). This is close to the effective index of refraction applied in this study for the WHOPS data analysis, such that non-hygroscopic bioparticles would correctly be measured at a GF of ∼ 1 by the WHOPS.

4.1.3 Hygroscopicity comparison between airborne WHOPS and ground-based HTDMA measurements

The ground stations were equipped with HTDMAs which measured GF-PDFs at RH = 90 % in the dry diameter range below 230 nm. Since SPC is located in the valley only the new ML and later the fully developed ML could be measured, while MTC, situated on a mountain, probes air in the RL in the morning and the fully developed ML later in the day. The fact that the fully developed ML extends to altitudes higher than the MTC site was previously reported by Van Dingenen et al. (2005). Figure 7 provides the WHOPS and HTDMA GF-PDFs measured on the Zeppelin, in SPC and MTC divided into results for the new ML, the RL and the fully developed ML. Note that the WHOPS cannot reliably detect particles with GF < 1.5 and D_{dry} = 300 nm, as described in Rosati et al. (2015). Thus, no information is available from the WHOPS measurement on the number fraction and properties of the 300 nm particles with GF < 1.5.

ACPD
15, 9445–9505, 2015

Figure 7a illustrates the averaged GF-PDFs in the newly forming ML. A first comparison between the two dry sizes probed by the WHOPS reveals a strong resemblance of the GF-PDF shapes for GF > 1.5, except for a small shift towards larger GFs for the smaller particle size. This suggests that hygroscopic particles of these two sizes have a similar chemical composition. When, however, comparing to the $HTDMA_{SPC}$ obvious differences appear: The distinct mode at GF ∼ 1 seen by the WHOPS for the 500 nm particles is much smaller in the HTDMA results. This might be due to the fact, that possible explanations for the non-hygroscopic particles (described in Sect. 4.1.2) are more probable for the larger size investigated by the WHOPS. In addition, the dominant hygroscopic mode is centered at smaller GFs in the HTDMA GF-PDF, which causes a smaller mean GF and κ value compared to the WHOPS. This is seen in the mean κ values, listed in Table 2, which have been derived from the mean GFs using Eq. (3). It is very unlikely that these differences solely arise from the size-dependent particle composition since upper accumulation mode particles at 200 and 300 nm are expected to be similar. The chemical analysis, which will be discussed in Sect. 4.1.4, reveals a nitrate mass fraction of ∼ 22 % in the non-refractory PM_1 composition. Ammonium nitrate is semi-volatile and prone to evaporation artifacts. Gysel et al. (2007) provided strong evidence for ammonium nitrate artifacts during HTDMA measurements, which resulted in underestimated hygroscopic GFs. The HTDMAs employed in SPC and MTC featured smaller residence times in the range between 10–15 s which should minimize nitrate evaporation losses, however, they can still not be fully excluded. GF measurements done by the WHOPS are most likely less susceptible to ammonium nitrate evaporation, as the residence time in the dry part of the instrument is lower due to higher flow rates. Thus, part of the difference between the ground-based SPC-HTDMA and the airborne WHOPS in the new ML could potentially be caused by artifacts in the HTDMA, which results in a small bias of measured GFs. Another possible reason could be that the particles at the ground (measured in the surface layer) and at 100 m a.g. were not exactly the same due to e.g. direct influences by local emissions.

ACPD
15, 9445–9505, 2015

Figure 7b depicts the averaged GF-PDFs in the RL. For GF > 1.5 the WHOPS results for both sizes agree well, again indicating similar chemical composition of particles with dry diameters of 300 and 500 nm. The GF-PDFs measured by the HTDMA at the MTC site are similar to the results from the airborne WHOPS measurements. Differences in the fine structure of the GF-PDFs should not be over-interpreted, as they are influenced by the data inversion algorithms for both instruments. Larger discrepancies are visible for the non-hygroscopic fraction. The HTDMA at MTC measured the GF-PDF for particles with a diameter of 230 nm, which could be too small to have a substantial fraction of dust or biological particles that are known to be non-hygroscopic and more abundant at larger sizes. Besides, MTC is situated at a much higher elevation than the Zeppelin NT was flying and its location is approximately 100 km southeast of SPC, therefore different airmasses could be present which lead to additional discrepancies.

Figure 7c displays the results for the fully developed ML. There is again little difference between the results for the two sizes probed by the WHOPS, as for the other two layers. The fully developed ML was probed by the HTDMA at both sites. The number fraction of non-hygroscopic particles is again smaller compared to the WHOPS, while the dominant hygroscopic mode is similar except for small differences in its position, which is also reflected in the mean κ values listed in Table 2.

4.1.4 Composition – hygroscopicity closure

The WHOPS measurements indicate distinct differences in hygroscopic particle properties between the probed layers in the PBL. Here we examine which chemical components cause these differences and whether closure is achieved between measured particle hygroscopicity and that calculated from chemical composition. Figure 8 depicts the PM_1 mass fractions of carbonaceous and inorganic aerosol components, as well as the mean PM_1 mass concentrations for the SPC ground station (Fig. 8a and b) and the altitude levels probed during the Zeppelin NT flights (Fig. 8c–f). Organic and inorganic species were always measured by an AMS, while eBC was measured by a MAAP and an aethalometer at the SPC site and on board the Zeppelin NT, respectively.

ACPD
15, 9445–9505, 2015

Figure 8a, c and e illustrate results for the early morning hours. At this time of day, the highest PM_1 concentrations were measured in new ML with mean values of 22 and 20 $\mu g\,m^{-3}$ at the ground site and ~ 100 m a.g., respectively. This is expected as most emissions from the ground, which accumulated during the night, are trapped in the new ML. The mean PM_1 concentrations in the RL at ~ 700 m a.g., which is decoupled from the emissions at the ground, were substantially lower (15 $\mu g\,m^{-3}$). These vertical gradients in aerosol concentration disappeared and aerosol loadings dropped as the new ML evolved to a fully developed ML in the course of the day, which resulted in stronger dilution and better vertical mixing of fresh emissions from the ground. This is confirmed by the results of the afternoon flights, when consistently 12–13 $\mu g\,m^{-3}$ were measured at both flight levels and the ground station (Fig. 8b, d and f).

Overall, organic compounds were with 43 to 62 % by mass the largest fraction of PM_1, while the sum of inorganic species contributed between 29 and 48 % (Fig. 8). The eBC mass fraction remained constantly below 12 % and chloride was always negligible with less than 1 %. During IHP1/2 a clear difference between the mass fractions in the new ML with a high nitrate fraction of 20–22 % (Fig. 8a and c) and the RL with a nitrate contribution of only 5 % (Fig. 8e) were observed. This increased nitrate fraction in the new ML can be explained by the accumulation of nitrate species over night, which are formed in the nocturnal surface layer and are then entrained into the new ML after sunrise. The eBC fraction was slightly higher in the new ML compared to the RL, whereas the organics and sulfate fractions were substantially lower. During the afternoon flights (IHP4/5/6; Fig. 8b, d and f) in the fully developed ML, the differences in chemical composition between different altitudes disappeared as they did for the aerosol loading. The mass fractions of all species were comparable at the ground and the two flight altitudes and also very similar to those in the RL probed in the morning.

Several AMS campaigns at SPC previously determined the chemical composition at ground level. A springtime campaign presented in Saarikoski et al. (2012) revealed a nitrate peak during the break-up of the nocturnal boundary layer, consistent with our observations, suggesting local sources of nitrate. In contrast, sulfate concentrations

ACPD
15, 9445–9505, 2015

stayed constant throughout the day, thus indicating small local influence, again consistent with our results. Previous airborne AMS measurements showed high ammonium nitrate concentrations in the Po Valley plume, thus indicating large nitrogen oxide and ammonium sources in the Po Valley region (Crosier et al., 2007).

A quantitative closure study between measured chemical composition and hygroscopic properties was done with the approach described in Sect. 3. For this purpose, Eq. (5) was used to calculated the κ value corresponding to the measured chemical composition from AMS and aethalometer. Resulting κ values averaged for the different layers are listed in Table 2. Inorganic species are strongly hygroscopic, while organics and BC are only weakly hygroscopic and non-hygroscopic, respectively (Table 1). Consequently, the hygroscopicity of a mixture increases with increasing inorganic fraction. This explains why the highest composition-derived κ values are obtained for the new ML (44–48 % inorganic mass fraction), both for the ground-based and airborne measurements at 100 m a.g., while those for the RL (35 % inorganic mass fraction) and the fully developed ML (29–30 % inorganic mass fraction) are distinctly lower. The differences in the inorganic fraction between the different layers are mainly caused by the variability of the nitrate fraction. Thus, the high nitrate mass fraction in the new ML is responsible for the increased particle hygroscopicity in this layer. Figure 4 (time-resolved data) and Table 2 (mean values for layers) further show that closure between composition-derived κ values and WHOPS-derived κ values is achieved within experimental uncertainty.

The κ values derived from the HTDMA measurement at the SPC site are significantly lower than the corresponding composition-derived κ values for the measurements in the new ML (Table 2). This disagreement might be caused as the result of ammonium nitrate evaporation artifacts in the HTDMA, as already speculated in Sect. 4.1.3. During previous measurements at the SPC site, Bialek et al. (2014) observed peaks of the nitrate mass fraction without a concurrent peak in particle hygroscopicity. It was suggested that this might have been due to the presence of organo-nitrates or organic

ACPD
15, 9445–9505, 2015

coating on particles, which both lead to low hygroscopic growth. However, also evaporation artifacts could potentially play a role.

4.1.5 Comparison of hygroscopicity results with previous campaigns

The aerosol hygroscopic properties reported in this study were measured on 20 June 2012, a predominately cloudless summer day with low wind speeds. To better understand whether this case study is representative of typical conditions in the Po Valley in the summer season, a comparison is made with literature data from previous campaigns that covered longer time periods. Mean κ values determined with different methods and at different sites are shown in Fig. 9. Only measurements taken in the fully developed ML are included in the averages (for the literature data, the time of day between 12:00 and 17:00 LT is assumed to be representative of the fully developed ML). Vertical gradients of aerosol properties are minimal in the fully developed ML. This ensures comparability between the measurements taken at different altitudes. Previous hygroscopicity measurements in the summer season were carried out with HTDMAs at MTC (Van Dingenen et al., 2005), at SPC (Bialek et al., 2014) and Ispra (Adam et al., 2012). Ispra is located at 45°49′ N, 8°38′ E at 209 m a.s.l. approximately 60 km north of Milan at the north-end of the Po Valley.

All mean κ values shown in Fig. 9 fall into the rather narrow range between 0.18 and 0.28, independent of location, method and dry sizes. These medium-low κ values can be explained with organic fractions of 50 % or larger (see e.g. Fig. 8). Additionally, the temporal variability is small, such that the range κ = 0.11–0.33 includes all data points within ±1 SD of the mean values. This means that a κ value of ∼ 0.22 is a good approximation for the aerosol hygroscopic properties in the fully developed ML in the Po Valley in summertime. Such approximations can for example be useful, when estimating the cloud condensation nuclei activity at times or sites without concurrent hygroscopicity or composition measurements. A closer look into the spatial pattern reveals that the summertime aerosol at Ispra and MTC seems to be slightly more hygroscopic than in the SPC area.

ACPD
15, 9445–9505, 2015

The close agreement between aerosol hygroscopic properties observed in this study with available literature data from previous studies suggests that our case study is indeed representative of the Po Valley summertime aerosol. Combined with the results shown in Figs. 4–7 follows that ground based measurements taken in the afternoon at sites in the valley plain are representative of aerosol properties over the whole vertical extent of the fully developed ML, whereas they may be representative of only a shallow layer at other times of day.

4.2 Netherlands campaign

Here we present the findings of a Zeppelin flight on 24 May 2012 near the CESAR ground station in the Netherlands (Fig. 1). We performed a set of height profiles between approximately 11:00 and 14:00 LT, including longer legs at the following for altitudes: ∼ 100, 300, 500 and 700 m a.g. The first height profile (NHP1) was performed from ∼ 11:30–12:45 LT and the second height profile (NHP2) from ∼ 12:45–13:50 LT. The wind direction was predominately from north-east and the wind speed on average between ∼ 3 and ∼ 4.5 $m\,s^{-1}$. Therefore, the probed airmasses were most probably originating from the continent and likely with some local/regional influence due to low wind speeds. Figure 10 displays the time series of the flight altitude, estimated mixing layer height, relative humidity and potential temperature (Θ). During the whole flight relatively high RH dominated (40–80 %). The pattern of Θ reveals a vertical layering during the first profile, showing a clear difference at ∼ 700 m a.g. compared to the lower altitudes. A similar but less pronounced vertical structure in the potential temperature can also be seen at the beginning of the second profile. A very similar development of the mixing layer height is captured by data calculated from a Ceilometer. This indicates that indeed we managed to fly above the new ML during the first profile at 700 m a.g. However, since the change in Θ and the vertical distance to the ML height are rather small, it is not clear whether the RL or the entrainment zone between the new ML and the RL were probed. The second profile at 700 m a.g. was most likely in the threshold range between new ML, entrainment zone and RL. In contrast to the flights in Italy, the

ACPD
15, 9445–9505, 2015

ones in the Netherlands started later in the day and therefore the ML had more time to develop. This is one reason why most measurements during this flight were within the new ML while none of them was for certain in the RL.

4.2.1 Hygroscopicity and mixing state inferred from WHOPS measurements

Figure 11 shows particle hygroscopicity measured by the WHOPS. The same flight pattern was repeated once. No substantial differences can be observed neither as a function of altitude nor of time. Absence of vertical gradients is expected for all measurements at altitudes of 500 m a.g. or lower, which have been shown to be within the almost fully to fully developed ML. The fact that the first measurement at 700 m a.g. is also similar to all others indicates either that the entrainment zone between the new ML and RL was probed or that the aerosol properties in the RL were similar to those in the new ML. As no temporal trend was observed, Table 3 presents directly mean values averaged over both profiles for each flight altitude separately. GF values between 1.84 and 1.93 at RH = 95 % were measured, which corresponds to κ values between between 0.25–0.29. It seems that particle hygroscopicity increases slightly but systematically with increasing altitude. One possible explanation for this could be temperature dependent partitioning of ammonium nitrate (which is hygroscopic; see Table 1). Morgan et al. (2010a) previously reported an increasing nitrate fraction with increasing altitude in the Cabauw area, which was observed between measurements at the ground site and $\sim$ 2000 m a.g.

The GF-PDFs for a dry particle diameter of 500 nm averaged for each altitude are presented in Fig. 12. GF-PDFs between a GF of 0.9 up to 3.2 are visible. This implies the presence of particles that differ substantially in their hygroscopic properties between each other. The GF-PDFs measured at the four altitudes are very similar. This shows that also the aerosol mixing state is equal within the ML. In order to further investigate the mixing state, the GF-PDFs were split into three hygroscopicity classes, and the corresponding number fractions of particles are shown in Fig. 13 (the hygroscopicity classes were equally chosen as for the flight data from Italy shown in Fig. 6).

ACPD
15, 9445–9505, 2015

The aerosol was externally mixed during the whole flight with very stable number fractions in each hygroscopicity class at any time and altitude. The dominant fraction of particles was more hygroscopic (GF > 1.5) making up 82 % (72–89 %) of the particles, while 12 % (7–18 %) were non-hygroscopic (GF < 1.1) and only 6 % (1–9 %) of the particles fell into the range 1.1 < GF < 1.5. As many as 12 % non-hygroscopic particles on average is, despite being only about half of the corresponding fraction observed in the Po Valley, higher than expected. Potential candidates for these particles are dust, biological material or tar balls as already discussed in Sect. 4.1.2. The influence of dust should be smaller in the Netherlands compared to the Po Valley. We do not have any evidence of specific influence from potential sources of tar balls. This would leave biological material as an important contributor to the non-hygroscopic particles at D_{dry} = 500 nm. However, we do not have any supporting data to corroborate or discard this speculation.

4.2.2 Composition – hygroscopicity closure

Unfortunately, the AMS data is not available for this Zeppelin flight due to an instrument failure. However, at the ground site an AMS measurement was successfully performed. The chemical composition results at the ground station in Cabauw (see Fig. 14) indicate organics as the major fraction describing 47 and 51 % of the aerosol, during NHP1 and NHP2, respectively. During both profiles nitrate constitutes the second most abundant fraction accounting for 24 and 17 %, while sulfate makes up 10 and 13 % of the total mass. The eBC fraction measured at the ground contributes to 7–9 % of the total mass.

The approach described in Sect. 3 is used to compare the ground based composition measurements with the airborne hygroscopicity measurements in a quantitative manner. For this purpose, Eq. (5) is used to calculated the κ value corresponding to the measured chemical composition. The resulting κ value is 0.28, which agrees well within uncertainty with the WHOPS-derived κ value of 0.25 in the lowermost flight level at 100 m a.g. (see Table 3). Such good agreement cannot necessarily be expected, as for example fresh and aged sea salt components are not quantitatively detected by the

ACPD
15, 9445–9505, 2015

AMS. However, in the next section we show that the sea salt influence was likely low during the flight presented in this study.

4.2.3 Comparison of hygroscopicity results with previous campaigns

Airborne hygroscopicity measurements from a different Zeppelin flight in Cabauw have previously been reported in (Rosati et al., 2015) as a first example of airborne operation of the WHOPS. This flight was characterized by sampling two distinct air mass types with and without substantial influence of sea salt aerosol. Figure 15 provides a comparison of the results from (Rosati et al., 2015) with those of this study. The general features of the three GF-PDFs are comparable, all featuring a minor peak at GF ∼ 1 and a dominant broad mode peaking in the range GF = 1.9–2.5. A clear increase of particles with GF > 2.5 was observed by (Rosati et al., 2015) for the airmass with sea salt (SS) influence, as opposed to the airmass without sea salt (non-SS) influence. The results of this study more closely resemble the latter airmass, thus indicating that this flight was not substantially influenced by sea salt.

The aerosol hygroscopic properties reported in this study were measured in a continental airmass with likely some local/regional influence due to low wind speeds. To better understand whether this case study is representative of typical conditions in the Cabauw region, a comparison is made with literature data from previous campaigns. Mean κ values determined with different methods and for different airmass types are shown in Fig. 16. Only measurements taken in the fully developed ML are included in the averages (for the literature data, the time of day between 12:00 and 17:00 LT is assumed to be representative of the fully developed ML). Vertical gradients of aerosol properties are minimal in the fully developed ML. This ensures comparability between the airborne and ground based measurements. Zieger et al. (2011) determined the hygroscopic properties with both, a HTDMA and a humidified nephelometer ("Wet-Neph"). To assess differences between days with and without influence from sea salt aerosol, two days were selected here from their comprehensive data set: 8 July 2009 is representative for SS and 14 July 2009 for non-SS conditions. The airborne WHOPS

ACPD
15, 9445–9505, 2015

measurements from (Rosati et al., 2015) are also separately shown for SS and non-SS influence. The literature data in Fig. 16 clearly show that the aerosol at Cabauw is more hygroscopic under the influence of sea salt aerosol, with mean κ values between 0.33 and 0.5. The spread between the three methods is partially related to the increasing sea salt fraction with increasing particle size, as shown by Zieger et al. (2011). For conditions without SS influence, literature reports lower κ values between 0.23 and 0.31, which matches the results of this study well. Thus, the flight of this study can be considered to be representative of the ML in the Cabauw area when airmasses without substantial SS influence prevail. When κ values from the overview presented in Fig. 15 are used as estimates for aerosol hygroscopicity at the Cabauw site for times when no direct or indirect measurement is available, then the uncertainty of the estimate can be reduced by distinguishing between air masses with and without SS influence if possible.

5 Conclusions

The night time and the morning PBL is often separated in layers which contain particles of different age and chemical history. Vertical profiles of chemical composition and hygroscopic growth factors were performed to relate particle properties to the layering of the atmosphere during the development of the mixing layer. The campaigns were performed in the Po Valley in Italy, near the ground station of San Pietro Capofiume (SPC) and in the Netherlands close to Cabauw.

During the flight on 20 June 2012 close to SPC different layers could be explored: the residual layer (RL), the new mixed layer (ML) and the ML when it was fully developed. Major differences in chemical composition and hygroscopicity were found in the first hours of the day when the new ML entrains air from the nocturnal boundary layer. During this time PM_1 nitrate concentrations amount to 20 % of the total aerosol mass leading to hygroscopicity parameters (κ) of 0.34 and 0.27 measured by the WHOPS (at D_{dry} = 500 nm) and retrieved from the PM_1 chemical composition, respectively. This

ACPD
15, 9445–9505, 2015

nitrate peak can be explained by the accumulation of nitrate species during the night which are diluted in the new ML during the day. κ values in the RL and fully developed ML are comparable for the physical and chemical analysis approach. Both measurements yield lower values compared to the new ML around 0.19. During the last flight hours only the fully developed ML could be probed where no characteristic altitude dependence was found. Ground based observations compare well to low-altitude, airborne results. Therefore, during the early development of the ML it is not possible to infer altitude specific data from surface measurements. In contrast, ground-based data can yield reasonable results for the fully developed ML. The mixing state of the aerosols was investigated using the WHOPS, revealing an external mixture over the whole day at all altitudes. The major fraction (67 %) experienced GF > 1.5, while 22 % were non-hygroscopic (GF < 1.1). There is evidence that the fraction of non-hygroscopic aerosols is associated with mineral dust and biological particles.

Airmasses in the Netherlands probed on 24 May 2012 did not feature altitude dependent aerosol properties which can be explained by the fact that only the fully developed ML or the entrainment zone between ML and RL were sampled. The hygroscopic fraction (GF > 1.5) was more pronounced than in the Po Valley amounting to 82 % of the total aerosol. Again an externally mixed aerosol was found, where 12 % of the particles showed GF < 1.1 when exposed to high RH. The mean κ value found by the WHOPS measurements was of 0.28, while ground based measurements yielded lower values of 0.24. These results coincided within the errors and the higher values found with the WHOPS could possibly be explained by a higher fractional contribution of semi-volatile and more hygroscopic aerosol species at higher altitudes.

Comparing the two different sites it seems that the non-hygroscopic aerosol fraction (GF < 1.1) plays a more important role in the Po Valley which could be explained by enhanced Saharan dust intrusions which affect the bigger size range. Hysplit calculations support this hypothesis observing dust intrusions even in the lowest layer of 100 m a.g. on this specific flight day. On the other hand the fraction of particles with GF > 1.5 in the fully developed ML is considerably higher in Cabauw compared to the Po Valley.

ACPD
15, 9445–9505, 2015

Overall chemical composition measurements feature the organics fraction as the most dominant one both in Italy and the Netherlands, describing approximately 50 % of the total aerosol mass. The effective index of refraction reached values of 1.43 and 1.42 for the 500 nm particles in Italy and the Netherlands, respectively. This coincides well with literature data for air masses with predominant organic contribution.

Acknowledgements. This work was supported by the EC project PEGASOS, funded by the European Commission under the Framework Programme 7 (FP7-ENV-2010-265148). We thank all PEGASOS participants for the excellent team work during the campaigns. Additionally we thank F. Holland for the analysis and maintenance of all meteorological and GPS data on the Zeppelin and R. Tillmann for his contributions to the paper. Also, we thank I. Pap and K. Weinhold for their help in maintaining the MAAP instrument at the SPC ground site. M. Gysel was supported by the ERC under grant 615922-BLACARAT. The field work at the ground-based stations was partly funded by Regione Emilia Romagna as part of the SUPERSITO project (DRG no. 428/10). The research leading to these results has also received funding from the European Union's Seventh Framework Programme's (FP7/2007-2013) BACCHUS project (grant agreement no. 603445). Part of the in-situ aerosol observations used in this study have received funding from the European Union Seventh Framework Programme (FP7/2007-2013) ACTRIS under grant agreement no. 262254.

References

Adam, M., Putaud, J. P., Martins dos Santos, S., Dell'Acqua, A., and Gruening, C.: Aerosol hygroscopicity at a regional background site (Ispra) in Northern Italy, Atmos. Chem. Phys., 12, 5703–5717, doi:10.5194/acp-12-5703-2012, 2012. 9470

Alexander, D. T. L., Crozier, P. A., and Anderson, J. R.: Brown carbon spheres in east asian outflow and their optical properties, Science, 321, 833–836, doi:10.1126/science.1155296, 2008. 9464

Allan, J. D., Delia, A. E., Coe, H., Bower, K. N., Alfarra, M., Jimenez, J. L., Middlebrook, A. M., Drewnick, F., Onasch, T. B., Canagaratna, M. R., Jayne, J. T., and Worsnop, D. R.: A gener-

ACPD
15, 9445–9505, 2015

alised method for the extraction of chemically resolved mass spectra from Aerodyne aerosol mass spectrometer data, J. Aerosol Sci., 35, 909–922, doi:10.1016/j.jaerosci.2004.02.007, 2004. 9456
Angelini, F., Barnaba, F., Landi, T., Caporaso, L., and Gobbi, G.: Study of atmospheric aerosols and mixing layer by LIDAR, Radiat. Prot. Dosim., 137, 275–279, 2009. 9453
Balaev, A. E., Dvoretski, K. N., and Doubrovski, V. A.: Determination of refractive index of rod-shaped bacteria from spectral extinction measurements, Proceedings of the SPIE, 5068, 375–380, doi:10.1117/12.518853, 2003. 9465
Bialek, J., Dall Osto, M., Vaattovaara, P., Decesari, S., Ovadnevaite, J., Laaksonen, A., and O'Dowd, C.: Hygroscopic and chemical characterisation of Po Valley aerosol, Atmos. Chem. Phys., 14, 1557–1570, doi:10.5194/acp-14-1557-2014, 2014. 9469, 9470
Bohren, C. F. and Huffman, D. R.: Absorption and Scattering of Light by Small Particles, Wiley-VCH Verlag GmbH, New York, NY, USA, doi:10.1002/9783527618156.fmatter, 2007. 9454
Bond, T. C. and Bergstrom, R. W.: Light absorption by carbonaceous particles: an investigative review, Aerosol Sci. Tech., 40, 27–67, doi:10.1080/02786820500421521, 2006. 9463
Charrière, F., Cuche, E., Marquet, P., and Depeursinge, C.: Biological cell (pollen grain) refractive index tomography with digital holographic microscopy, Proceedings of the SPIE, 6090, p. 9008, doi:10.1117/12.645903, 2006. 9465
Collaud Coen, M., Weingartner, E., Apituley, A., Ceburnis, D., Fierz-Schmidhauser, R., Flentje, H., Henzing, J. S., Jennings, S. G., Moerman, M., Petzold, A., Schmid, O., and Baltensperger, U.: Minimizing light absorption measurement artifacts of the Aethalometer: evaluation of five correction algorithms, Atmos. Meas. Tech., 3, 457–474, doi:10.5194/amt-3-457-2010, 2010. 9457
Crosier, J., Allan, J. D., Coe, H., Bower, K. N., Formenti, P., and Williams, P. I.: Chemical composition of summertime aerosol in the Po Valley (Italy), northern Adriatic and Black Sea, Q. J. Roy. Meteor. Soc., 133, 61–75, doi:10.1002/qj.88, 2007. 9469
DeCarlo, P. F., Kimmel, J. R., Trimborn, A., Northway, M. J., Jayne, J. T., Aiken, A. C., Gonin, M., Fuhrer, K., Horvath, T., Docherty, K. S., Worsnop, D. R., and Jimenez, J. L.: Field-deployable, high-resolution, time-of-flight aerosol mass spectrometer, Anal. Chem., 78, 8281–8289, doi:10.1021/ac061249n, 2006. 9455
Decesari, S., Allan, J., Plass-Duelmer, C., Williams, B. J., Paglione, M., Facchini, M. C., O'Dowd, C., Harrison, R. M., Gietl, J. K., Coe, H., Giulianelli, L., Gobbi, G. P., Lanconelli, C., Carbone, C., Worsnop, D., Lambe, A. T., Ahern, A. T., Moretti, F., Tagliavini, E., Elste, T.,

ACPD
15, 9445–9505, 2015

Gilge, S., Zhang, Y., and Dall'Osto, M.: Measurements of the aerosol chemical composition and mixing state in the Po Valley using multiple spectroscopic techniques, Atmos. Chem. Phys., 14, 12109–12132, doi:10.5194/acp-14-12109-2014, 2014. 9464

Després, V., Huffman, J., Burrows, S., Hoose, C., Safatov, A., Buryak, G., Fröhlich-Nowoisky, J., Elbert, W., Andreae, M., Pöschl, U., and Jaenicke, R.: Primary biological aerosol particles in the atmosphere: a review, Tellus B, 64, 15598, doi:10.3402/tellusb.v64i0.15598, 2012. 9465

Di Giuseppe, F., Riccio, A., Caporaso, L., Bonafé, G., Gobbi, G., and Angelini, F.: Automatic detection of atmospheric boundary layer height using ceilometer backscatter data assisted by a boundary layer model, Q. J. Roy. Meteor. Soc., 138, 649–663, 2012. 9453

Duplissy, J., DeCarlo, P. F., Dommen, J., Alfarra, M. R., Metzger, A., Barmpadimos, I., Prevot, A. S. H., Weingartner, E., Tritscher, T., Gysel, M., Aiken, A. C., Jimenez, J. L., Canagaratna, M. R., Worsnop, D. R., Collins, D. R., Tomlinson, J., and Baltensperger, U.: Relating hygroscopicity and composition of organic aerosol particulate matter, Atmos. Chem. Phys., 11, 1155–1165, doi:10.5194/acp-11-1155-2011, 2011. 9449, 9459

Ferrero, L., Castelli, M., Ferrini, B. S., Moscatelli, M., Perrone, M. G., Sangiorgi, G., D'Angelo, L., Rovelli, G., Moroni, B., Scardazza, F., Močnik, G., Bolzacchini, E., Petitta, M., and Cappelletti, D.: Impact of black carbon aerosol over Italian basin valleys: high-resolution measurements along vertical profiles, radiative forcing and heating rate, Atmos. Chem. Phys., 14, 9641–9664, doi:10.5194/acp-14-9641-2014, 2014. 9455

Fierz-Schmidhauser, R., Zieger, P., Gysel, M., Kammermann, L., DeCarlo, P. F., Baltensperger, U., and Weingartner, E.: Measured and predicted aerosol light scattering enhancement factors at the high alpine site Jungfraujoch, Atmos. Chem. Phys., 10, 2319–2333, doi:10.5194/acp-10-2319-2010, 2010. 9464

Guyon, P., Boucher, O., Graham, B., Beck, J., Mayol-Bracero, O., Roberts, G., Maenhaut, W., Artaxo, P., and Andreae, M.: Refractive index of aerosol particles over the Amazon tropical forest during LBA-EUSTACH 1999, J. Aerosol Sci., 34, 883–907, doi:10.1016/S0021-8502(03)00052-1, 2003. 9455

Gysel, M., Crosier, J., Topping, D. O., Whitehead, J. D., Bower, K. N., Cubison, M. J., Williams, P. I., Flynn, M. J., McFiggans, G. B., and Coe, H.: Closure study between chemical composition and hygroscopic growth of aerosol particles during TORCH2, Atmos. Chem. Phys., 7, 6131–6144, doi:10.5194/acp-7-6131-2007, 2007. 9458, 9466

ACPD
15, 9445–9505, 2015

Gysel, M., McFiggans, G., and Coe, H.: Inversion of tandem differential mobility analyser (TDMA) measurements, J. Aerosol Sci., 40, 134–151, doi:10.1016/j.jaerosci.2008.07.013, 2009. 9455

Haeffelin, M., Angelini, F., Morille, Y., Martucci, G., Frey, S., Gobbi, G., Lolli, S., O'Dowd, C., Sauvage, L., Xueref-Rémy, I., Wastine, B., and Feist, D.: Evaluation of mixing-height retrievals from automatic profiling lidars and ceilometers in view of future integrated networks in Europe, Bound.-Lay. Meteorol., 143, 49–75, doi:10.1007/s10546-011-9643-z, 2012. 9453

Haij, M., Wauben, W., and Klein-Baltink, H.: Continuous mixing layer height determination using the LD-40 ceilometer: a feasibility study, KNMI Scientific Report 07-01, available at: http://www.knmi.nl/publications/fulltexts/200701_bsikmlh_wr200701.pdf, 2007. 9453

Herich, H., Kammermann, L., Gysel, M., Weingartner, E., Baltensperger, U., Lohmann, U., and Cziczo, D. J.: In situ determination of atmospheric aerosol composition as a function of hygroscopic growth, J. Geophys. Res.-Atmos., 113, D16213, doi:10.1029/2008JD009954, 2008. 9464

Herich, H., Tritscher, T., Wiacek, A., Gysel, M., Weingartner, E., Lohmann, U., Baltensperger, U., and Cziczo, D. J.: Water uptake of clay and desert dust aerosol particles at sub- and supersaturated water vapor conditions, Phys. Chem. Chem. Phys., 11, 7804–7809, doi:10.1039/b901585j, 2009. 9464

Hersey, S. P., Sorooshian, A., Murphy, S. M., Flagan, R. C., and Seinfeld, J. H.: Aerosol hygroscopicity in the marine atmosphere: a closure study using high-time-resolution, multiple-RH DASH-SP and size-resolved C-ToF-AMS data, Atmos. Chem. Phys., 9, 2543–2554, doi:10.5194/acp-9-2543-2009, 2009. 9450

Hersey, S. P., Craven, J. S., Metcalf, A. R., Lin, J., Lathem, T., Suski, K. J., Cahill, J. F., Duong, H. T., Sorooshian, A., Jonsson, H. H., Shiraiwa, M., Zuend, A., Nenes, A., Prather, K. A., Flagan, R. C., and Seinfeld, J. H.: Composition and hygroscopicity of the Los Angeles Aerosol: CalNex, J. Geophys. Res.-Atmos., 118, 3016–3036, doi:10.1002/jgrd.50307, 2013. 9450

Holmgren, H., Sellegri, K., Hervo, M., Rose, C., Freney, E., Villani, P., and Laj, P.: Hygroscopic properties and mixing state of aerosol measured at the high-altitude site Puy de Dôme (1465 m a.s.l.), France, Atmos. Chem. Phys., 14, 9537–9554, doi:10.5194/acp-14-9537-2014, 2014. 9450

ACPD
15, 9445–9505, 2015

IPCC: The Physical Science Basis. Contribution of Working Group I to the Fifth Assessment Report of the Intergovernmental Panel on Climate Change, Cambridge University Press, Cambridge, UK and New York, NY, USA, 2013. 9448

Jurányi, Z., Tritscher, T., Gysel, M., Laborde, M., Gomes, L., Roberts, G., Baltensperger, U., and Weingartner, E.: Hygroscopic mixing state of urban aerosol derived from size-resolved cloud condensation nuclei measurements during the MEGAPOLI campaign in Paris, Atmos. Chem. Phys., 13, 6431–6446, doi:10.5194/acp-13-6431-2013, 2013. 9463

Kamilli, K. A., Poulain, L., Held, A., Nowak, A., Birmili, W., and Wiedensohler, A.: Hygroscopic properties of the Paris urban aerosol in relation to its chemical composition, Atmos. Chem. Phys., 14, 737–749, doi:10.5194/acp-14-737-2014, 2014. 9450

Kammermann, L., Gysel, M., Weingartner, E., and Baltensperger, U.: 13-month climatology of the aerosol hygroscopicity at the free tropospheric site Jungfraujoch (3580 m a.s.l.), Atmos. Chem. Phys., 10, 10717–10732, doi:10.5194/acp-10-10717-2010, 2010. 9450

Kim, H. and Paulson, S. E.: Real refractive indices and volatility of secondary organic aerosol generated from photooxidation and ozonolysis of limonene, α-pinene and toluene, Atmos. Chem. Phys., 13, 7711–7723, doi:10.5194/acp-13-7711-2013, 2013. 9455

Kuwata, M., Zorn, S. R., and Martin, S. T.: Using elemental ratios to predict the density of organic material composed of carbon, hydrogen, and oxygen, Environ. Sci. Technol., 46, 787–794, doi:10.1021/es202525q, 2012. 9459, 9487

Laborde, M., Crippa, M., Tritscher, T., Jurányi, Z., Decarlo, P. F., Temime-Roussel, B., Marchand, N., Eckhardt, S., Stohl, A., Baltensperger, U., Prévôt, A. S. H., Weingartner, E., and Gysel, M.: Black carbon physical properties and mixing state in the European megacity Paris, Atmos. Chem. Phys., 13, 5831–5856, doi:10.5194/acp-13-5831-2013, 2013. 9463, 9464

Lance, S., Raatikainen, T., Onasch, T. B., Worsnop, D. R., Yu, X.-Y., Alexander, M. L., Stolzenburg, M. R., McMurry, P. H., Smith, J. N., and Nenes, A.: Aerosol mixing state, hygroscopic growth and cloud activation efficiency during MIRAGE 2006, Atmos. Chem. Phys., 13, 5049–5062, doi:10.5194/acp-13-5049-2013, 2013. 9463

Limsui, D., Carr, A. K., Thomas, M. E., Boggs, N. T., and Joseph, R. I.: Refractive index measurement of biological particles in visible region, Proceedings of the SPIE, 6954, 69540X-69540X-7, doi:10.1117/12.777648, 2008. 9465

Liu, B. Y. H., Pui, D. Y. H., Whitby, K. T., Kittelson, D. B., Kousaka, Y., and McKenzie, R. L.: Aerosol mobility chromatograph – new detector for sulfuric – acid aerosols, Atmos. Environ., 12, 99–104, doi:10.1016/0004-6981(78)90192-0, 1978. 9449

ACPD
15, 9445–9505, 2015

Mahowald, N., Albani, S., Kok, J. F., Engelstaeder, S., Scanza, R., Ward, D. S., and Flanner, M. G.: The size distribution of desert dust aerosols and its impact on the Earth system, Aeolian Research, 15, 53–71, doi:10.1016/j.aeolia.2013.09.002, 2014. 9464

McMurry, P. H. and Stolzenburg, M. R.: On the sensitivity of particle-size to relative humidity for los angeles aerosols, Atmos. Environ., 23, 497–507, doi:10.1016/0004-6981(89)90593-3, 1989. 9449

Middlebrook, A. M., Bahreini, R., Jimenez, J. L., and Canagaratna, M. R.: Evaluation of composition-dependent collection efficiencies for the Aerodyne aerosol mass spectrometer using field data, Aerosol Sci. Tech., 46, 258–271, doi:10.1080/02786826.2011.620041, 2012. 9456

Mie, G.: Beiträge zur Optik trüber Medien, speziell kolloidaler Metallösungen, Annalen der Physik, 330, 377–445, doi:10.1002/andp.19083300302, 1908. 9454

Morgan, W. T., Allan, J. D., Bower, K. N., Capes, G., Crosier, J., Williams, P. I., and Coe, H.: Vertical distribution of sub-micron aerosol chemical composition from North-Western Europe and the North-East Atlantic, Atmos. Chem. Phys., 9, 5389–5401, doi:10.5194/acp-9-5389-2009, 2009. 9449

Morgan, W. T., Allan, J. D., Bower, K. N., Esselborn, M., Harris, B., Henzing, J. S., Highwood, E. J., Kiendler-Scharr, A., McMeeking, G. R., Mensah, A. A., Northway, M. J., Osborne, S., Williams, P. I., Krejci, R., and Coe, H.: Enhancement of the aerosol direct radiative effect by semi-volatile aerosol components: airborne measurements in North-Western Europe, Atmos. Chem. Phys., 10, 8151–8171, doi:10.5194/acp-10-8151-2010, 2010a. 9449, 9472

Morgan, W. T., Allan, J. D., Bower, K. N., Highwood, E. J., Liu, D., McMeeking, G. R., Northway, M. J., Williams, P. I., Krejci, R., and Coe, H.: Airborne measurements of the spatial distribution of aerosol chemical composition across Europe and evolution of the organic fraction, Atmos. Chem. Phys., 10, 4065–4083, doi:10.5194/acp-10-4065-2010, 2010b. 9449

Müller, T., Henzing, J. S., de Leeuw, G., Wiedensohler, A., Alastuey, A., Angelov, H., Bizjak, M., Collaud Coen, M., Engström, J. E., Gruening, C., Hillamo, R., Hoffer, A., Imre, K., Ivanow, P., Jennings, G., Sun, J. Y., Kalivitis, N., Karlsson, H., Komppula, M., Laj, P., Li, S.-M., Lunder, C., Marinoni, A., Martins dos Santos, S., Moerman, M., Nowak, A., Ogren, J. A., Petzold, A., Pichon, J. M., Rodriquez, S., Sharma, S., Sheridan, P. J., Teinilä, K., Tuch, T., Viana, M., Virkkula, A., Weingartner, E., Wilhelm, R., and Wang, Y. Q.: Characterization and intercom-

ACPD
15, 9445–9505, 2015

parison of aerosol absorption photometers: result of two intercomparison workshops, Atmos. Meas. Tech., 4, 245–268, doi:10.5194/amt-4-245-2011, 2011. 9456

Petters, M. D. and Kreidenweis, S. M.: A single parameter representation of hygroscopic growth and cloud condensation nucleus activity, Atmos. Chem. Phys., 7, 1961–1971, doi:10.5194/acp-7-1961-2007, 2007. 9457, 9458

Petzold, A., and Schönlinner, M.: Multi-angle absorption photometry a new method for the measurement of aerosol light absorption and atmospheric black carbon, J. Aerosol Sci., 35, 421–441, doi:10.1016/j.jaerosci.2003.09.005, 2004. 9456

Petzold, A., Schloesser, H., Sheridan, P., Arnott, W., Ogren, J., and Virkkula, A.: Evaluation of multiangle absorption photometry for measuring aerosol light absorption, Aerosol Sci. Tech., 39, 40–51, doi:10.1080/027868290901945, 2005. 9456

Pratt, K. A. and Prather, K. A.: Aircraft measurements of vertical profiles of aerosol mixing states, J. Geophys. Res.-Atmos., 115, D11305, doi:10.1029/2009JD013150, 2010. 9449

Pósfai, M., Gelencsér, A., Simonics, R., Arató, K., Li, J., Hobbs, P. V., and Buseck, P. R.: Atmospheric tar balls: Particles from biomass and biofuel burning, J. Geophys. Res.-Atmos., 109, D06213, doi:10.1029/2003JD004169, 2004. 9464

Putaud, J.-P., Dingenen, R. V., Alastuey, A., Bauer, H., Birmili, W., Cyrys, J., Flentje, H., Fuzzi, S., Gehrig, R., Hansson, H., Harrison, R., Herrmann, H., Hitzenberger, R., Hüglin, C., Jones, A., Kasper-Giebl, A., Kiss, G., Kousa, A., Kuhlbusch, T., Löschau, G., Maenhaut, W., Molnar, A., Moreno, T., Pekkanen, J., Perrino, C., Pitz, M., Puxbaum, H., Querol, X., Rodriguez, S., Salma, I., Schwarz, J., Smolik, J., Schneider, J., Spindler, G., ten Brink, H., Tursic, J., Viana, M., Wiedensohler, A., and Raes, F.: A European aerosol phenomenology – 3: Physical and chemical characteristics of particulate matter from 60 rural, urban, and kerbside sites across Europe, Atmos. Environ., 44, 1308–1320, doi:10.1016/j.atmosenv.2009.12.011, 2010. 9452

Rosati, B., Wehrle, G., Gysel, M., Zieger, P., Baltensperger, U., and Weingartner, E.: The white-light humidified optical particle spectrometer (WHOPS) – a novel airborne system to characterize aerosol hygroscopicity, Atmos. Meas. Tech., 8, 921–939, doi:10.5194/amt-8-921-2015, 2015. 9451, 9453, 9455, 9460, 9465, 9474, 9475, 9504, 9505

Rose, D., Wehner, B., Ketzel, M., Engler, C., Voigtländer, J., Tuch, T., and Wiedensohler, A.: Atmospheric number size distributions of soot particles and estimation of emission factors, Atmos. Chem. Phys., 6, 1021–1031, doi:10.5194/acp-6-1021-2006, 2006. 9463

ACPD
15, 9445–9505, 2015

Rubach, F.: Aerosol Processes in the Planetary Boundary Layer: High resolution Aerosol Mass Spectrometry on a Zeppelin NT Airship, PhD thesis, Bergische Universität Wuppertal, Germany, 2013. 9456

Saarikoski, S., Carbone, S., Decesari, S., Giulianelli, L., Angelini, F., Canagaratna, M., Ng, N. L., Trimborn, A., Facchini, M. C., Fuzzi, S., Hillamo, R., and Worsnop, D.: Chemical characterization of springtime submicrometer aerosol in Po Valley, Italy, Atmos. Chem. Phys., 12, 8401–8421, doi:10.5194/acp-12-8401-2012, 2012. 9468

Schladitz, A., Mueller, T., Nowak, A., Kandler, K., Lieke, K., Massling, A., and Wiedensohler, A.: In situ aerosol characterization at Cape Verde Part 1: Particle number size distributions, hygroscopic growth and state of mixing of the marine and Saharan dust aerosol, Tellus B, 63, 531–548, doi:10.1111/j.1600-0889.2011.00569.x, 2011. 9464

Sjogren, S., Gysel, M., Weingartner, E., Alfarra, M. R., Duplissy, J., Cozic, J., Crosier, J., Coe, H., and Baltensperger, U.: Hygroscopicity of the submicrometer aerosol at the high-alpine site Jungfraujoch, 3580 m a.s.l., Switzerland, Atmos. Chem. Phys., 8, 5715–5729, doi:10.5194/acp-8-5715-2008, 2008. 9464

Sorooshian, A., Hersey, S. P., Brechtel, F. J., Corless, A., Flagan, R. C., and Seinfeld, J. H.: Rapid, size-resolved aerosol hygroscopic growth measurements: differential aerosol sizing and hygroscopicity spectrometer probe (DASH-SP), Aerosol Sci. Tech., 42, 445–464, doi:10.1080/02786820802178506, 2008. 9450

Stokes, R. H. and Robinson, R. A.: Interactions in aqueous nonelectrolyte solutions, I. Solute – solvent equilibria, J. Phys. Chem.-US, 70, 2126, doi:10.1021/j100879a010, 1966. 9458

Stull, R.: An Introduction to Boundary Layer Meteorology, Kluwer Academic Publisher, Dordrecht, the Netherlands, 1988. 9448

Swietlicki, E., Hansson, H. C., Hameri, K., Svenningsson, B., Massling, A., McFiggans, G., McMurry, P. H., Petaja, T., Tunved, P., Gysel, M., Topping, D., Weingartner, E., Baltensperger, U., Rissler, J., Wiedensohler, A., and Kulmala, M.: Hygroscopic properties of submicrometer atmospheric aerosol particles measured with H-TDMA instruments in various environments - a review, Tellus B, 60, 432–469, doi:10.1111/j.1600-0889.2008.00350.x, 2008. 9449, 9455

Topping, D. O., McFiggans, G. B., and Coe, H.: A curved multi-component aerosol hygroscopicity model framework: Part 1 – Inorganic compounds, Atmos. Chem. Phys., 5, 1205–1222, doi:10.5194/acp-5-1205-2005, 2005. 9459

Tritscher, T., Juranyi, Z., Martin, M., Chirico, R., Gysel, M., Heringa, M. F., DeCarlo, P. F., Sierau, B., Prevot, A. S. H., Weingartner, E., and Baltensperger, U.: Changes of hygro-

ACPD
15, 9445–9505, 2015

scopicity and morphology during ageing of diesel soot, Environ. Res. Lett., 6, 034026, doi:10.1088/1748-9326/6/3/034026, 2011. 9449, 9464

Van Dingenen, R., Putaud, J.-P., Martins-Dos Santos, S., and Raes, F.: Physical aerosol properties and their relation to air mass origin at Monte Cimone (Italy) during the first MINATROC campaign, Atmos. Chem. Phys., 5, 2203–2226, doi:10.5194/acp-5-2203-2005, 2005. 9465, 9470

Vlasenko, A., Sjogren, S., Weingartner, E., Stemmler, K., Gäggeler, H. W., and Ammann, M.: Effect of humidity on nitric acid uptake to mineral dust aerosol particles, Atmos. Chem. Phys., 6, 2147–2160, doi:10.5194/acp-6-2147-2006, 2006. 9464

Wagner, R., Ajtai, T., Kandler, K., Lieke, K., Linke, C., Müller, T., Schnaiter, M., and Vragel, M.: Complex refractive indices of Saharan dust samples at visible and near UV wavelengths: a laboratory study, Atmos. Chem. Phys., 12, 2491–2512, doi:10.5194/acp-12-2491-2012, 2012. 9464

Weingartner, E., Burtscher, H., and Baltensperger, U.: Hygroscopic properties of carbon and diesel soot particles, Atmos. Environ., 31, 2311–2327, doi:10.1016/S1352-2310(97)00023-X, 1997. 9463

Weingartner, E., Saathoff, H., Schnaiter, M., Streit, N., Bitnar, B., and Baltensperger, U.: Absorption of light by soot particles: determination of the absorption coefficient by means of aethalometers, J. Aerosol Sci., 34, 1445–1463, doi:10.1016/S0021-8502(03)00359-8, 2003. 9457

Wex, H., Petters, M. D., Carrico, C. M., Hallbauer, E., Massling, A., McMeeking, G. R., Poulain, L., Wu, Z., Kreidenweis, S. M., and Stratmann, F.: Towards closing the gap between hygroscopic growth and activation for secondary organic aerosol: Part 1 – Evidence from measurements, Atmos. Chem. Phys., 9, 3987–3997, doi:10.5194/acp-9-3987-2009, 2009. 9455

Wu, Z. J., Poulain, L., Henning, S., Dieckmann, K., Birmili, W., Merkel, M., van Pinxteren, D., Spindler, G., Müller, K., Stratmann, F., Herrmann, H., and Wiedensohler, A.: Relating particle hygroscopicity and CCN activity to chemical composition during the HCCT-2010 field campaign, Atmos. Chem. Phys., 13, 7983–7996, doi:10.5194/acp-13-7983-2013, 2013. 9450

Yamasoe, M. A., Kaufman, Y. J., Dubovik, O., Remer, L. A., Holben, B. N., and Artaxo, P.: Retrieval of the real part of the refractive index of smoke particles from Sun/sky measurements during SCAR-B, J. Geophys. Res.-Atmos., 103, 31893–31902, doi:10.1029/98JD01211, 1998. 9455

ACPD
15, 9445–9505, 2015

Zhang, R., Khalizov, A. F., Pagels, J., Zhang, D., Xue, H., and McMurry, P. H.: Variability in morphology, hygroscopicity, and optical properties of soot aerosols during atmospheric processing, P. Natl. Acad. Sci. USA, 105, 10291–10296, doi:10.1073/pnas.0804860105, 2008. 9464

Zieger, P., Weingartner, E., Henzing, J., Moerman, M., de Leeuw, G., Mikkilä, J., Ehn, M., Petäjä, T., Clémer, K., van Roozendael, M., Yilmaz, S., Frieß, U., Irie, H., Wagner, T., Shaiganfar, R., Beirle, S., Apituley, A., Wilson, K., and Baltensperger, U.: Comparison of ambient aerosol extinction coefficients obtained from in-situ, MAX-DOAS and LIDAR measurements at Cabauw, Atmos. Chem. Phys., 11, 2603–2624, doi:10.5194/acp-11-2603-2011, 2011. 9450, 9474, 9475, 9505

ACPD
15, 9445–9505, 2015

Table 1. κ values and densities for pure compounds used for the prediction of aerosol hygroscopicity based on AMS and Aethalometer or MAAP measurements.

Compound	Density ρ [kg m^{-3}]	κ (95 %, 500 nm)
$(NH_4)_2SO_4$	1769	0.458
NH_4HSO_4	1780	0.575
H_2SO_4	1830	0.687
NH_4NO_3	1720	0.629
eBC	2000	0.000
organics	1233*	0.110

* Mean value retrieved throughout the campaign with the Kuwata et al. (2012) parametrization.

ACPD
15, 9445–9505, 2015

Table 2. Mean GF and κ values for IHP1/2 and IHP4/5/6 with respective accuracies. κ_{chem} is the calculated κ using the AMS and Aethalometer measurements on board of the Zeppelin NT or AMS/MAAP combination at the ground. Besides, results for two different altitudes and the corresponding layers probed are mentioned. Additionally, the size at which the measurements are performed is stated.

Zeppelin					
			WHOPS		AMS + Aethalometer
Size	Altitude	Layer	GF(95 %) 500 nm	κ_{WHOPS} 500 nm	κ_{chem} PM_1
IHP1/2	100 m	new ML	1.88(±0.19)	0.34(±0.12)	0.27(±0.06)
	700 m	RL	1.61(±0.16)	0.19(±0.07)	0.21(±0.05)
IHP4/5/6	100 m	fully developed ML	1.48(±0.15)	0.14(±0.06)	0.19(±0.04)
	700 m	fully developed ML	1.65(±0.17)	0.21(±0.08)	0.19(±0.04)

Ground Stations		San Pietro Capofiume		Monte Cimone
		AMS + MAAP	HTDMA	HTDMA
Size		κ_{chem} PM_1	κ_{HTDMA} 200 nm	κ_{HTDMA} 230 nm
IHP1/2	new ML	0.31(±0.08)	0.19(±0.04)*	
	RL			0.23(±0.05)*
IHP4/5/6	fully developed ML	0.21(±0.06)	0.18(±0.04)*	0.25(±0.05)*

* HTDMA uncertainty calculated assuming ±2 % accuracy in the RH measurement.

ACPD
15, 9445–9505, 2015

Table 3. Mean GF and κ values for NHP1/2 with respective accuracies are presented. For the WHOPS measurements at four different altitudes are shown. κ_{chem} is calculated from the Cabauw ground site combining AMS and MAAP results.

Zeppelin			
		WHOPS	
Size	Altitude	GF(95 %) 500 nm	κ_{WHOPS} 500 nm
NHP1/2	100 m	1.84(±0.18)	0.25(±0.09)
	300 m	1.91(±0.19)	0.28(±0.10)
	500 m	1.92(±0.19)	0.29(±0.10)
	700 m	1.93(±0.19)	0.29(±0.10)

Ground Station	Cabauw
	AMS + MAAP
Size	κ_{chem} PM_1
NHP1/2	0.28(±0.06)

ACPD
15, 9445–9505, 2015

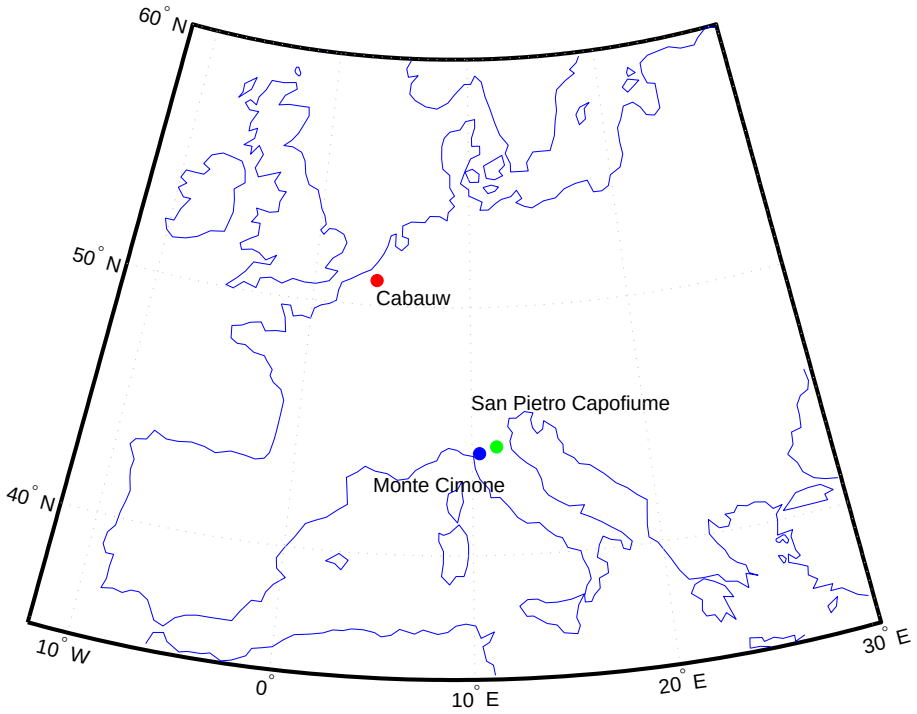

Figure 1. Map showing the different measurement sites in Europe: Cabauw located in the Netherlands (red dot) and San Pietro Capofiume (green dot) and Monte Cimone (blue dot) located in the Po Valley in Italy.

ACPD
15, 9445–9505, 2015

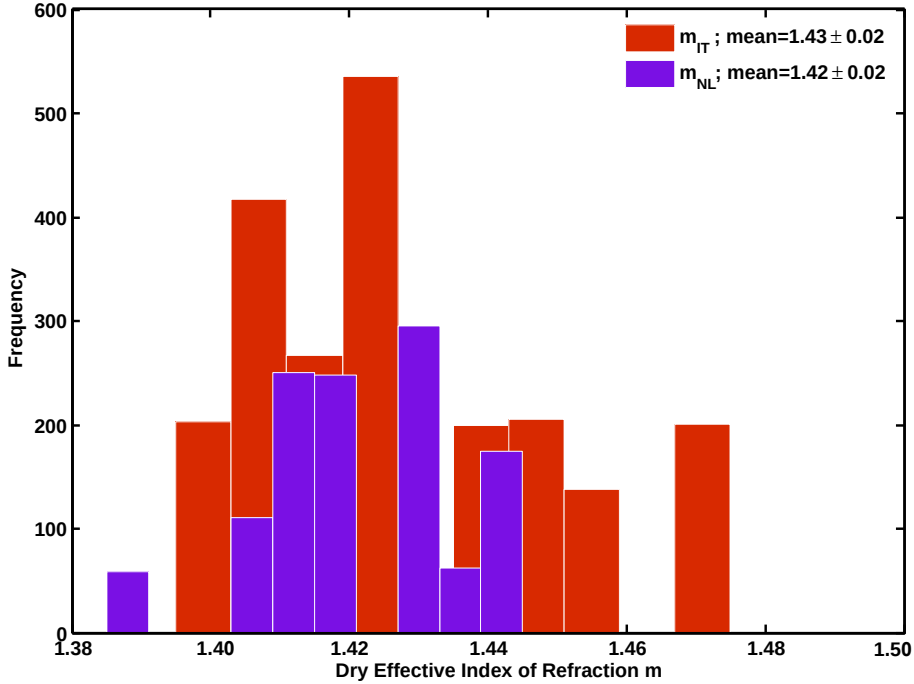

Figure 2. Retrieved dry effective index of refraction m for the flight in the Po Valley (m_{IT}, dark red bars) and the flight in the Netherlands (m_{NL}, violet bars) for particles with dry diameters of D_{dry} = 500 nm. Additionally mean values and their temporal variability are presented for both sites.

ACPD
15, 9445–9505, 2015

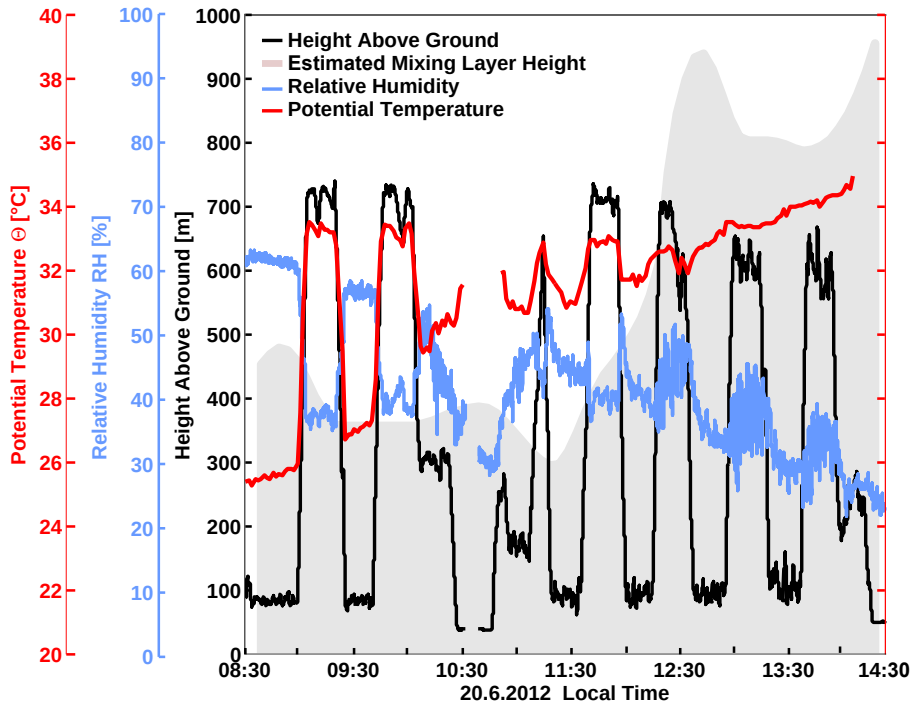

Figure 3. Overview of the flight on 20 June 2012 near San Pietro Capofiume ground station (Po Valley, Italy). In black the flight altitude and in gray the estimated mixing layer height, determined from Ceilometer – Lidar measurements, are presented. The red and blue lines show the potential temperature Θ and RH profiles, respectively.

ACPD
15, 9445–9505, 2015

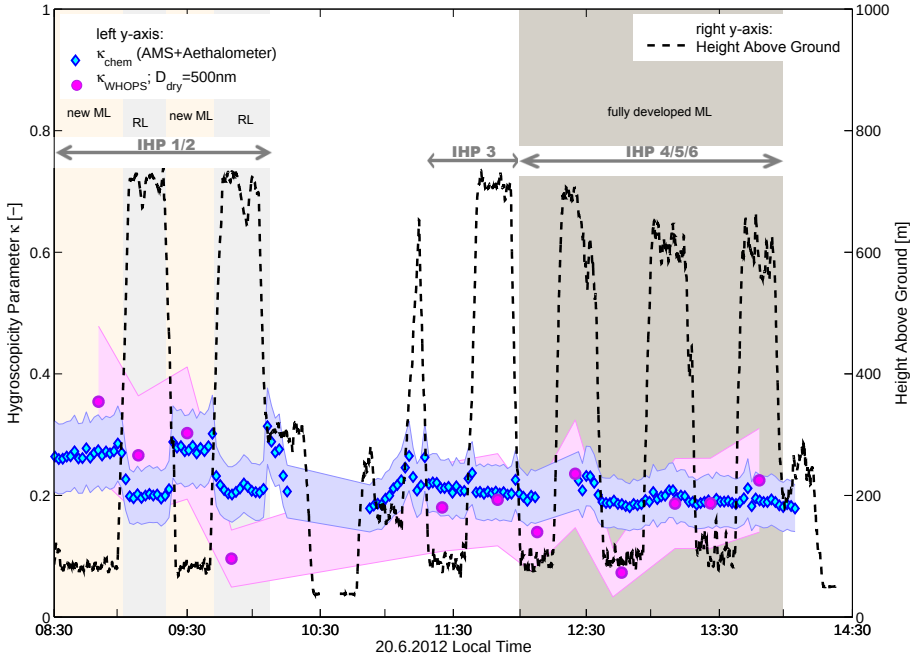

Figure 4. Time series of κ values on the 20 June 2012 in Italy. Results from chemical composition (κ_{chem}; green diamonds), and WHOPS for a dry selected diameter of 500 nm (κ_{WHOPS}; red dots) are shown. The shaded areas depict the measurement accuracy. The dashed line shows the flight altitude, while the gray, dashed rectangle indicates the break for refueling. In addition, the times for IHP1/2, IHP3 and IHP4/5/6 are indicated. The colored areas refer to the layer which was probed at that altitude.

ACPD
15, 9445–9505, 2015

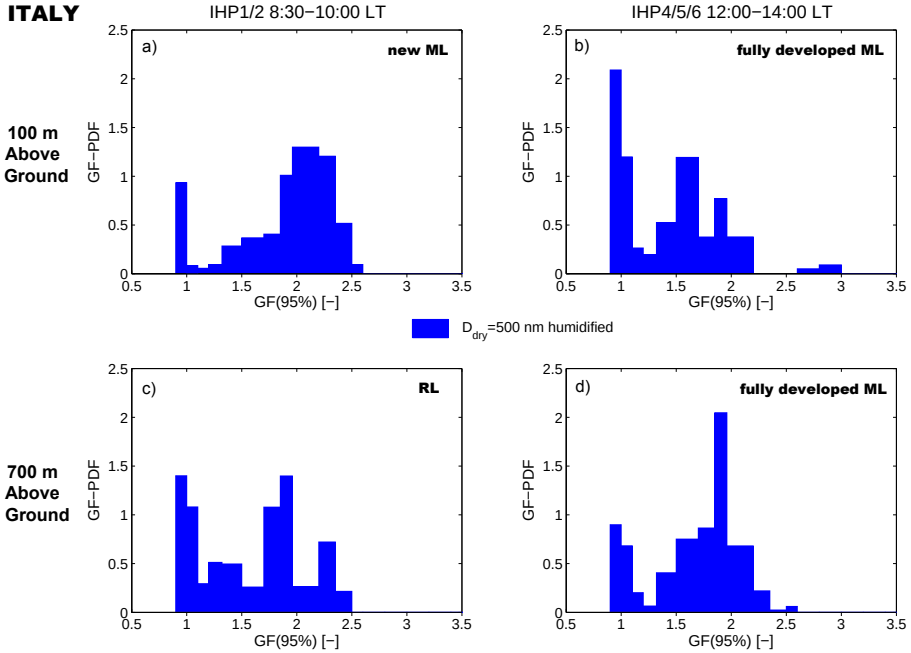

Figure 5. GF-PDFs during 20 June 2012 in Italy: profile IHP1/2 was flown between 08:30 and 10:00 LT and IHP4/5/6 between 12:00 and 14:00 LT; the blue area displays the GF-PDFs for a selected dry diameter of 500 nm. (**a** and **b**) illustrate the results at approximately 100 m a.g. and (**c** and **d**) for approximately 700 m a.g.

ACPD
15, 9445–9505, 2015

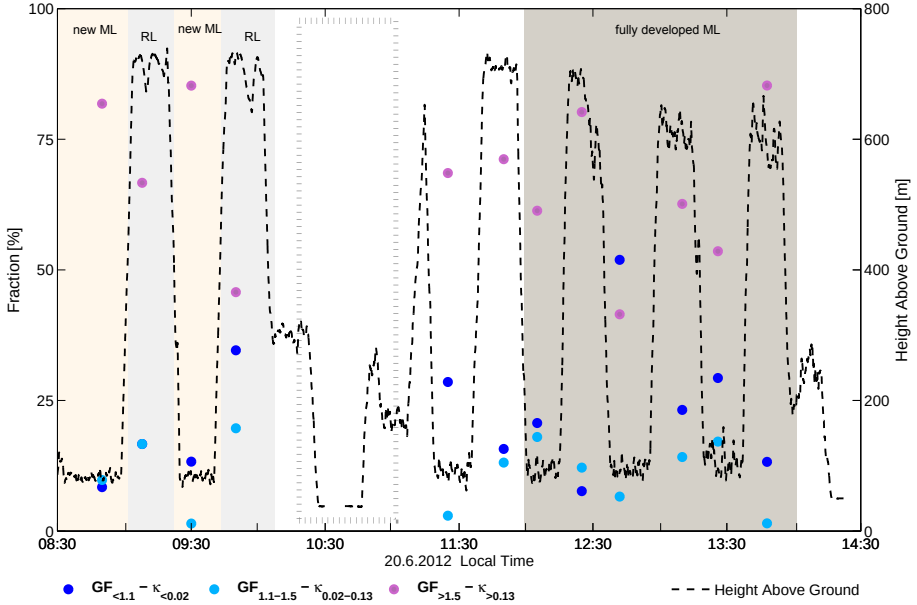

Figure 6. Time series of the mixing state of the aerosol particles (with D_{dry} = 500 nm) for the height profiles in Italy on 20 June 2012. Particles are classified into three hygroscopicity categories according to their GF: GF < 1.1, 1.1 < GF < 1.5, GF > 1.5, in blue, light blue and pink respectively; these are equivalent to $\kappa < 0.02$, $0.02 < \kappa < 0.13$ and $\kappa > 0.13$. The black, dashed line denotes the flight altitude and the gray rectangle illustrates the time of the refuel break. The colored areas refer to the layer which was probed at that altitude.

ACPD
15, 9445–9505, 2015

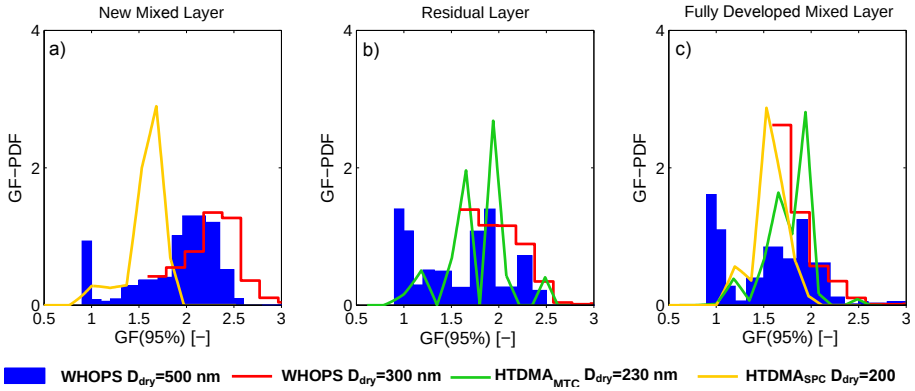

Figure 7. GF-PDF comparison between WHOPS and HTDMA subdivided for different layers: the new mixed layer, the residual layer and the fully developed mixed layer.

ACPD
15, 9445–9505, 2015

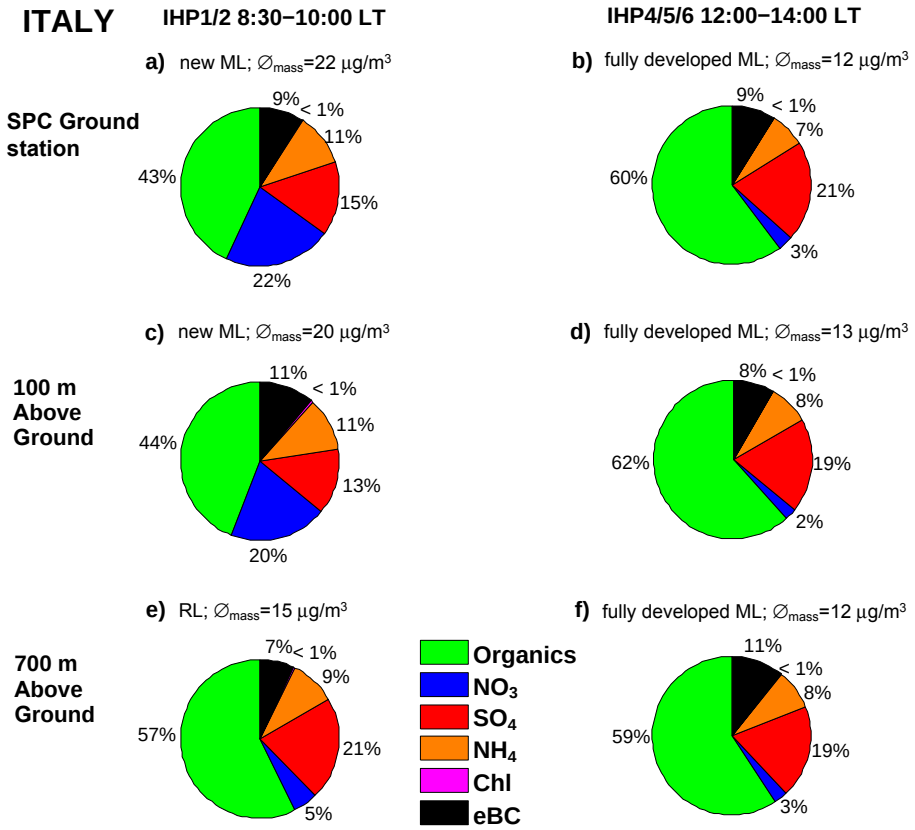

Figure 8. PM_1 chemical composition results during the flight on 20 June 2012 in Italy. **(a** and **b)** show the mass fractions measured by AMS and MAAP at San Pietro Capofiume ground station; **(a)** was recorded during IHP1/2 whereas **(b)** was measured during IHP4/5/6. **(c–f)** depict the mass fractions measured by AMS and Aethalometer on the Zeppelin. **(c** and **e)** illustrate the results for the first height profiles, **(c)** at 100 and **(e)** at 700 m a.g., while **(d** and **f)** show the results for IHP4/5/6 for 100 and 700 m a.g., respectively.

ACPD
15, 9445–9505, 2015

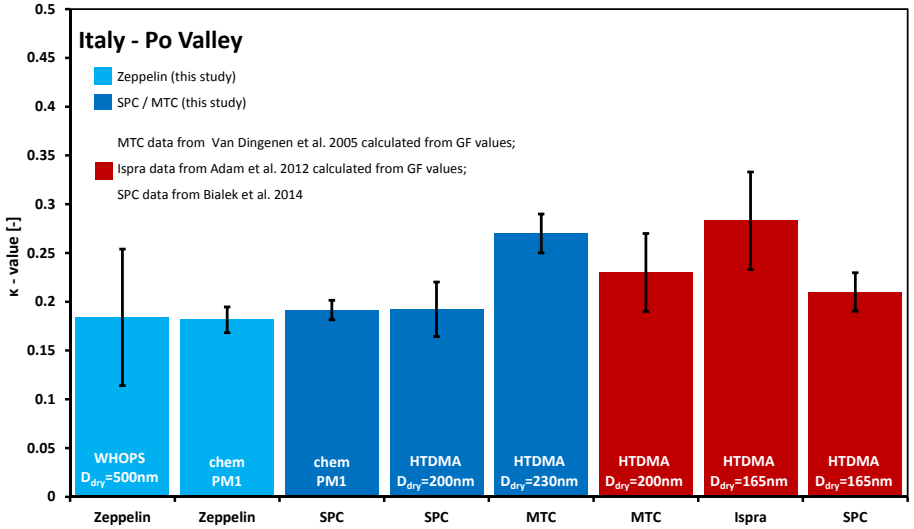

Figure 9. Intercomparison of mean κ values measured in this study at different locations in the Po Valley on 20 June 2012 (blue bars) compared with literature data from this area (red bars). κ values are either derived from measured hygroscopic growth factors or chemical composition. Only results for the fully developed ML, when vertical gradients of aerosol properties are minimal, are included in the averages. This ensures comparability between the measurements taken at different altitudes. The error bars indicate the temporal variability of the observed κ values (1 SD).

ACPD
15, 9445–9505, 2015

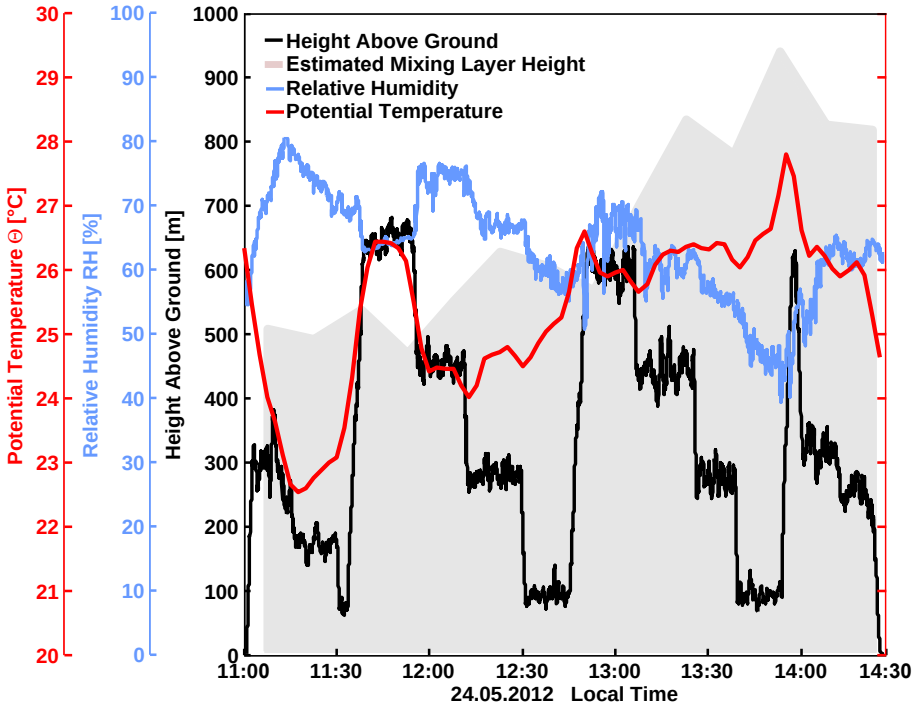

Figure 10. Overview of the flight on 24 May 2012 near Cabauw CESAR station in the Netherlands. In black the flight altitude and in gray the estimated mixing layer height, inferred from Ceilometer measurements, are presented. The red and blue lines show the potential temperature Θ and RH profiles, respectively.

ACPD
15, 9445–9505, 2015

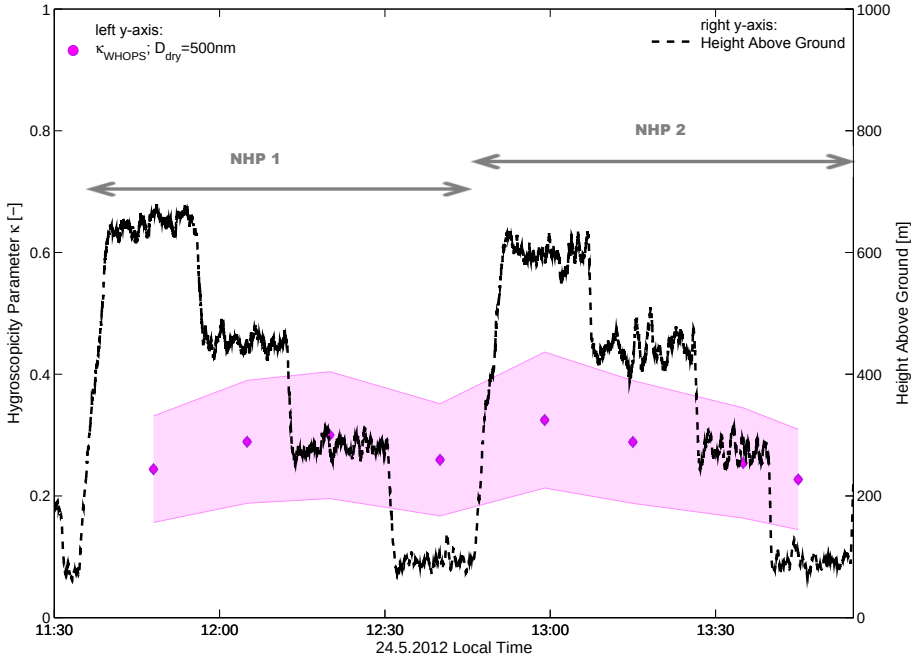

Figure 11. Time series of κ values retrieved during the flight on 24 May 2012. WHOPS results for a dry diameter of 500 nm are presented. The measurement accuracy is shown as the shaded area. Additionally, the flight altitude is indicated.

ACPD
15, 9445–9505, 2015

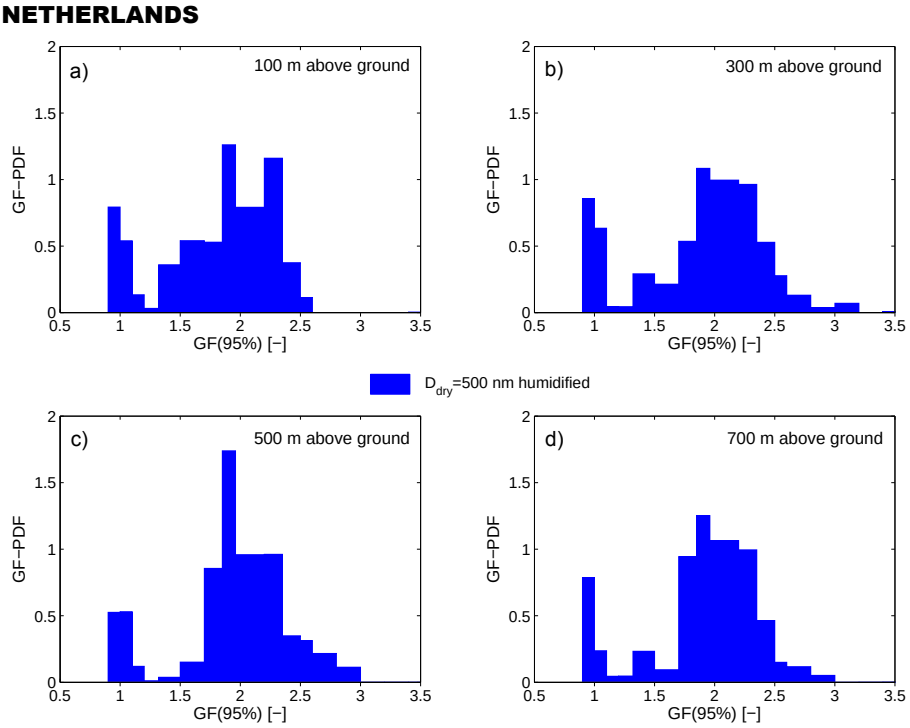

Figure 12. GF-PDFs recorded at Cabauw on 24 May 2012 at four different altitudes: approximately 100, 300, 500 and 700 m a.g. seen in panels **(a–d)**, respectively. Every curve is the mean over the two flown profiles NHP1 and NHP2.

ACPD
15, 9445–9505, 2015

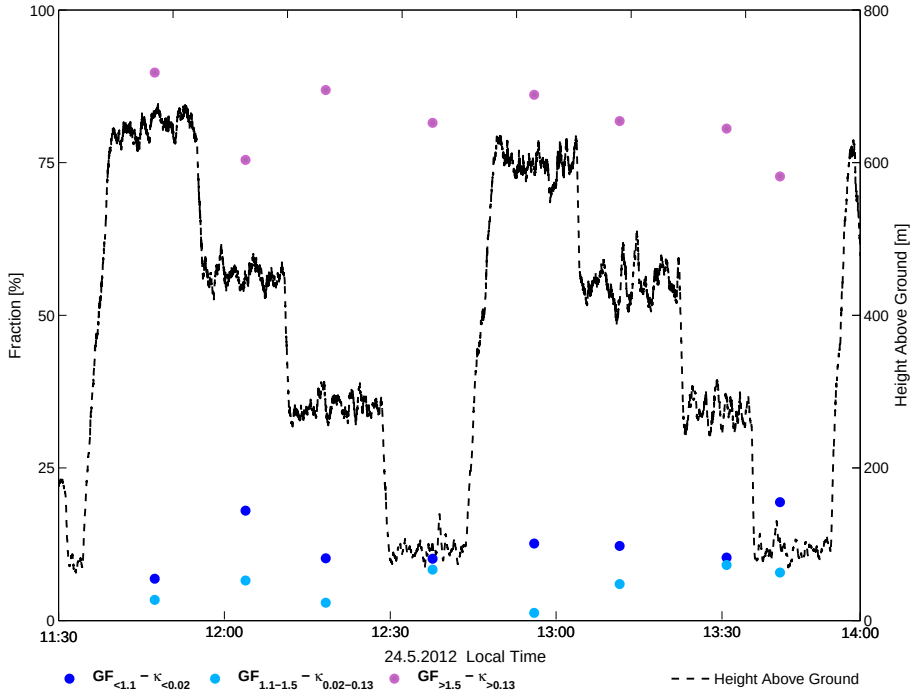

Figure 13. Time evolution of the mixing state of the aerosol particles (with D_{dry} = 500 nm) for the height profiles at Cabauw on 24 May 2012. Particles are classified into three hygroscopicity categories according to their GF (equally defined as for Fig. 6): GF < 1.1, 1.1 < GF < 1.5, GF > 1.5, in blue, light blue and pink respectively; these correspond to $\kappa < 0.02$, $0.02 < \kappa < 0.13$ and $\kappa > 0.13$.

ACPD
15, 9445–9505, 2015

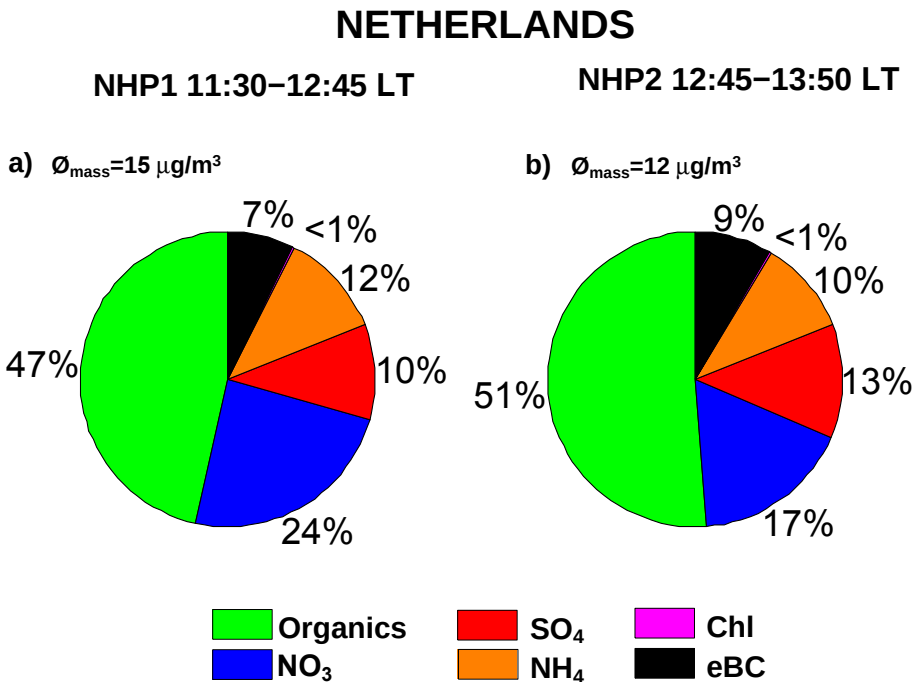

Figure 14. Ground measurements of the aerosol particle chemical composition at the Cabauw tower during NHP1 and NHP2 on 24 May 2012. AMS and MAAP results are combined for the total aerosol mass. Also, the averaged mass concentrations during the profile periods are stated.

ACPD
15, 9445–9505, 2015

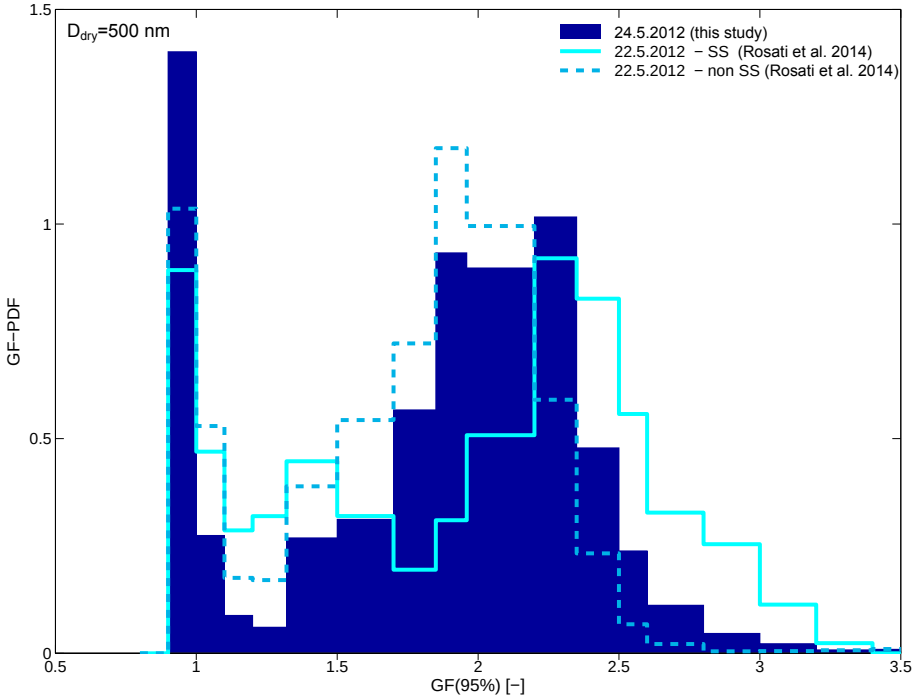

Figure 15. Comparison of GF-PDFs of particles with D_{dry} = 500 nm recorded with the Zeppelin mounted WHOPS during flights around Cabauw on 24 May 2012 (this study) and on 22 May 2012 (Rosati et al., 2015).

ACPD
15, 9445–9505, 2015

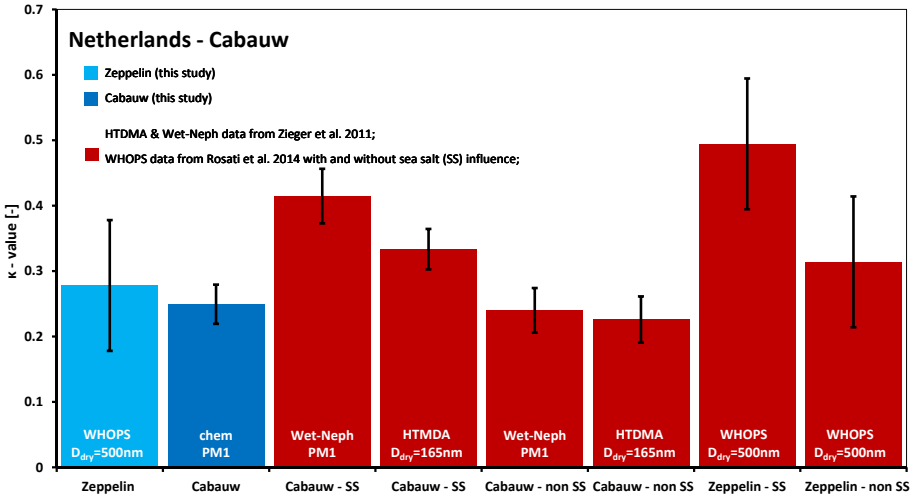

Figure 16. Intercomparison of mean κ values and their temporal variability measured on board of the Zeppelin NT (light blue bar) and at the ground (dark blue bar) during the PEGASOS campaign on 24 May 2012 in the Netherlands. Additionally results from two separate campaigns reported in the literature are shown (red bars). For the flight described in Rosati et al. (2015) two different bars are presented dividing results in sea salt (SS) and non-sea salt (non-SS) influenced periods. In the same way results from Zieger et al. (2011) are split in SS and non-SS periods for measurements performed with two different techniques.

ACPD
15, 9445–9505, 2015